

An observational test for correlations between cosmic rays and magnetic fields

Rodion Stepanov^{1,2,3*}, Anvar Shukurov¹, Andrew Fletcher¹, Rainer Beck⁴,
Laura La Porta^{4,6}, Fatemeh Tabatabaei⁵

¹*School of Mathematics and Statistics, Newcastle University, Newcastle upon Tyne, NE1 7RU, UK*

²*Institute of Continuous Media Mechanics, Academy of Sciences, Korolyov str. 1, Perm 614013, Russia*

³*Department of Applied Mathematics and Mechanics, National Research Polytechnic University of Perm, Komsomolskii Av. 29, 614990, Perm, Russia*

⁴*Max-Planck Institut für Radioastronomie, Auf dem Hügel 69, Bonn D-53121, Germany*

⁵*Max Planck Institut für Astronomie, Königstuhl 17, Heidelberg D-69117, Germany*

⁶*Institute of Geodesy and Geoinformation, University of Bonn, Nussallee 17, 53115 Bonn, Germany*

Accepted Received; in original form ...

ABSTRACT

We derive the magnitude of fluctuations in total synchrotron intensity in the Milky Way and M33, from both observations and theory under various assumption about the relation between cosmic rays and interstellar magnetic fields. Given the relative magnitude of the fluctuations in the Galactic magnetic field (the ratio of the rms fluctuations to the mean magnetic field strength) suggested by Faraday rotation and synchrotron polarization, the observations are inconsistent with local energy equipartition between cosmic rays and magnetic fields. Our analysis of relative synchrotron intensity fluctuations indicates that the distribution of cosmic rays is nearly uniform at the scales of the order of and exceeding 100 pc, in contrast to strong fluctuations in the interstellar magnetic field at those scales. A conservative upper limit on the ratio of the the fluctuation magnitude in the cosmic ray number density to its mean value is 0.2–0.4 at scales of order 100 pc. Our results are consistent with a mild anticorrelation between cosmic-ray and magnetic energy densities at these scales, in both the Milky Way and M33. Energy equipartition between cosmic rays and magnetic fields may still hold, but at scales exceeding 1 kpc. Therefore, we suggest that equipartition estimates be applied to the observed synchrotron intensity smoothed to a linear scale of kiloparsec order (in spiral galaxies) to obtain the cosmic ray distribution and a large-scale magnetic field. Then the resulting cosmic ray distribution can be used to derive the fluctuating magnetic field strength from the data at the original resolution. The resulting random magnetic field is likely to be significantly stronger than existing estimates.

Key words: cosmic rays – magnetic fields – galaxies: ISM – galaxies: magnetic fields – radio continuum: galaxies – radio continuum: general

1 MOTIVATION AND BACKGROUND

The concept of energy equipartition between cosmic rays and magnetic fields and similar assumptions such as pressure equality (Longair 1994; Beck & Krause 2005; Arbutina et al. 2012) are often used in the analysis and interpretation of radio astronomical observations. This idea was originally suggested in order to estimate the magnetic field and cosmic ray energies of the source *as a whole* (Burbidge 1956b,a), from a measurement of the synchrotron brightness of a radio source. A physically attractive feature of the

equipartition state is that it approximately minimizes the total energy of the radio source.

The energy density of cosmic rays is mainly determined by their proton component, whereas the synchrotron intensity depends on the number density of relativistic electrons. Therefore, in order to estimate the magnetic field energy, an assumption needs to be made about the ratio of the energy densities of the relativistic protons and electrons; the often adopted value for this ratio is 100, as suggested by Milky Way data (Beck & Krause 2005). This ratio is adopted to be unity in applications to galaxy clusters, radio galaxies and active objects (Carilli & Taylor 2002).

However, more recently this concept has been extended to large-scale trends in synchrotron intensity and to local energy densities at sub-kiloparsec scales in well-resolved radio sources, such

* E-mail: rodion@icmm.ru (RS); anvar.shukurov@ncl.ac.uk (AS); andrew.fletcher@ncl.ac.uk (AF); rbeck@mpifr-bonn.mpg.de (RB); laporta@mpifr-bonn.mpg.de (LLP); taba@mpia.de (FT)

as spiral galaxies (e.g., Beck et al. 2005; Beck 2007; Chyży 2008; Tabatabaei et al. 2008; Fletcher et al. 2011). Another important application of the equipartition hypothesis, first suggested by Parker (1966, 1969, 1979), is to the hydrostatic equilibrium of the interstellar gas. Here magnetic and cosmic ray pressures are assumed to be in a constant ratio, in practice taken to be unity. This application appeals to equipartition (or, more precisely, pressure equality) at larger scales of the order of kiloparsec. The spatial relation between fluctuations in magnetic field and cosmic rays is crucial for a proposed method to measure magnetic helicity in the ISM (Oppermann et al. 2011; Volegova & Stepanov 2010).

The physical basis of the equipartition assumption remains elusive. Since cosmic rays are confined within a radio source by magnetic fields, it seems natural to expect that the two energy densities are somehow related: if the magnetic field energy density ϵ_B is smaller than that of the cosmic rays, ϵ_{cr} , the cosmic rays would be able to ‘break through’ the magnetic field and escape; whereas a larger magnetic energy density would result in the accumulation of cosmic rays. Thus, the system is likely to be self-regulated to energy equipartition, $\epsilon_B \approx \epsilon_{cr}$. A slightly different version of these arguments refers to the equality of the two pressures,¹ giving $\epsilon_B \approx \frac{1}{3}\epsilon_{cr}$.

However plausible one finds these arguments, it is difficult to substantiate them. In particular, models of cosmic ray confinement suggest that the cosmic ray diffusion tensor depends on the *ratio* $(\delta B/B_0)^2$, where δB is the magnitude of magnetic field fluctuations at a scale equal to the proton gyroradius and B_0 is the mean magnetic field (e.g., Berezhinskii et al. 1990). The magnetic field strength can determine the streaming velocity of cosmic rays via the Alfvén speed, but the theory of cosmic ray propagation and confinement relates ϵ_{cr} to the intensity of cosmic ray sources rather than to the local magnetic field strength. Despite their uncertain basis, equipartition arguments remain popular as they provide ‘reasonable’ estimates of magnetic fields in radio sources, and also because they often offer the only practical way to obtain such estimates.

Equipartition between cosmic rays and magnetic fields can rarely be tested observationally. Chi & Wolfendale (1993) used γ -ray observations of the Magellanic clouds to calculate the energy density of cosmic rays independently of the equipartition assumption. They further calculated magnetic energy density from radio continuum data at a wavelength of about $\lambda 12$ cm. The resulting magnetic energy density is two orders of magnitude larger than that of cosmic rays, and Chi & Wolfendale (1993) argue that the discrepancy cannot be removed by assuming a proton-to-electron ratio for cosmic rays different from the standard value of 100 (see, however, Pohl 1993). More recently, however, Mao et al. (2012) analysed *Fermi* Large Area Telescope observations of the LMC (Abdo et al. 2010) and concluded that the equipartition assumption does not appear to be violated.

An independent estimate of magnetic field strength can be obtained for synchrotron sources of high surface brightness (e.g., active galactic nuclei) where the relativistic plasma absorbs an observable lower-frequency part of the radio emission (synchrotron self-absorption). Then the magnetic field strength can be estimated

from the frequency, the flux density and the angular size of the synchrotron source at the turnover frequency (Sligh 1963; Williams 1963; Scheuer & Williams 1968). Scott & Readhead (1977) and Readhead (1994) concluded, from low-frequency observations of compact radio sources whose angular size can be determined from interplanetary scintillations, that there is no significant evidence of strong departures from equipartition. In the sources with strong synchrotron self-absorption in their sample, the total energy is within a factor of 10 above the minimum energy. Orienti & Dallacasa (2008) observed, using VLBI, five young, very compact radio sources to suggest that magnetic fields in them are quite close to the equipartition value. Physical conditions in spiral galaxies are quite different from those in compact, active radio sources, and departures from equipartition by a factor of several in terms of magnetic field strength would be quite significant in the context of spiral galaxies.

Here we test the equipartition hypothesis using another approach (see also Stepanov et al. 2009). We calculate the relative magnitude of fluctuations in synchrotron intensity using model random magnetic field and cosmic ray distributions with a prescribed degree of cross-correlations. When the results are compared with observations, it becomes clear that local energy equipartition is implausible as it would produce stronger fluctuations of the synchrotron emissivity than are observed. Instead, the observed synchrotron intensity fluctuations suggest weak variations in the cosmic ray number density or an anticorrelation between cosmic rays and magnetic fields, perhaps indicative of pressure equilibrium. We conclude that local energy equipartition is unlikely in spiral galaxies at the integral scale of the fluctuations, of order 100 pc. We discuss the dynamics of cosmic rays to argue in favour of equipartition at larger scales of order 1 kpc, comparable to the scale of the mean magnetic field and to the cosmic-ray diffusion scale.

The paper is organized as follows. In Section 2 we discuss the relative strengths of the mean and fluctuating magnetic field in the Milky Way and M33. In Section 3 we use observational data to estimate the magnitude of synchrotron intensity variations at high galactic latitudes in the Milky Way and in the outer parts of M33. Theoretical models for synchrotron intensity fluctuations, allowing for controlled levels of cross-correlation between the magnetic field and cosmic ray distributions, are developed analytically in Section 4 and numerically in Section 5: readers who are interested only in our results may wish to skip these rather mathematical sections. Section 6 presents an interpretation of the observational data in terms of the theoretical models; here we estimate the cross-correlation coefficient between magnetic and cosmic-ray fluctuations. In Section 7 we briefly discuss cosmic ray propagation models from the viewpoint of relation between the cosmic ray and magnetic field distributions. Our results are discussed in Section 8 and Appendix A contains the details of some of our calculations.

2 THE MAGNITUDE OF FLUCTUATIONS IN INTERSTELLAR MAGNETIC FIELDS

The ratio of the fluctuating-to-mean synchrotron intensity in the interstellar medium (ISM) is sensitive to the relative distributions of cosmic ray electrons and magnetic fields and hence to the extent that energy equipartition may hold locally: the synchrotron emission will fluctuate strongly if equipartition holds pointwise, i.e., if the number density of cosmic ray electrons is increased where the local magnetic field is stronger. (We assume that cosmic ray elec-

¹ It is useful to carefully distinguish between what can be called ‘pressure equality’ and ‘pressure equilibrium’: the former refers to the case where magnetic fields and cosmic rays have equal pressures locally, whereas the latter describes the situation where the sum of the two (or more) pressure contributions does not vary in space.

trons and heavier relativistic particles are similarly distributed – see Section 8 for the justification.)

Interstellar magnetic fields are turbulent, with the ratio of the random magnetic field to its mean component known from observations of Faraday rotation, independently of the equipartition assumption. Denoting the standard deviation of the turbulent magnetic field by $\sigma_b^2 = \overline{B^2} - B_0^2$ and the mean field strength as $B_0 = |\overline{\mathbf{B}}|$, where bar denotes appropriate averaging (usually volume or line-of-sight averaging), the relative fluctuations in magnetic field strength in the Solar vicinity of the Milky Way is estimated as (Ruzmaikin et al. 1988; Ohno & Shibata 1993; Beck et al. 1996)

$$\delta_b^2 = \left(\frac{\sigma_b}{B_0}\right)^2 \simeq 3-10. \quad (1)$$

Similar estimates result from radio observations of nearby spiral galaxies where the degree of polarization of the integrated emission at 4.8 GHz is a few per cent, with a range $p \simeq 0.01-0.18$ (Stil et al. 2009). These data are affected by beam depolarization, so they only give upper limits for δ_b^2 . More typical values of the fractional polarisation in spiral galaxies are $p = 0.01-0.05$ within spiral arms and 0.1 on average. The degree of polarization at short wavelengths, where Faraday rotation is negligible, can be estimated as (Burn 1966; Sokoloff et al. 1998)

$$p = p_0 \frac{B_{0\perp}^2}{B_{0\perp}^2 + \frac{2}{3}\sigma_b^2} \quad (2)$$

where $B_{0\perp}$ is the strength of the large-scale magnetic field in the sky plane, the intrinsic degree of polarisation $p_0 \approx 0.75$, and the random magnetic field is assumed to be isotropic, $b_{\perp}^2 = \frac{2}{3}\sigma_b^2$. This yields

$$\delta_b^2 \simeq \frac{3}{2} \left(\frac{p_0}{p} - 1\right) \gtrsim 4 \quad \text{for } p < 0.2 \quad (3)$$

in a good agreement with the estimate (1) for the Milky Way data obtained from Faraday rotation measures. For $p = 0.05-0.1$, we obtain $\delta_b^2 \simeq 10-20$.

It is important to note that Eq. (3) has been obtained assuming that the cosmic ray number density n_{cr} is uniform, so that all the beam depolarization is attributed solely to the fluctuations in magnetic field. Under local equipartition, $n_{\text{cr}} \propto B^2$, Sokoloff et al. (1998, their Eq. (28)) calculated the degree of polarization at short wavelengths to be

$$p = p_0 \frac{1 + \frac{7}{3}\delta_b^2}{1 + 3\delta_b^2 + \frac{10}{9}\delta_b^4}.$$

As might be expected, this expression leads to a smaller δ_b for a given p/p_0 than Eq. (2):

$$\delta_b^2 \approx \frac{2p_0}{p} \quad \text{for } \frac{p}{p_0} \ll 1, \quad (4)$$

so that

$$\delta_b^2 \simeq 15 \quad \text{for } p = 0.1.$$

Since local equipartition between cosmic rays and magnetic fields maximizes beam depolarization, this is clearly a lower estimate of δ_b .

2.1 Anisotropic fluctuations

The above estimates apply to statistically isotropic random magnetic fields. However, the random part of the interstellar magnetic

field can be expected to be anisotropic at scales of order 100 pc, e.g., due to shearing by the galactic differential rotation, streaming motions and large-scale compression. Synchrotron emission arising in an anisotropic random magnetic field is polarized (Laing 1980; Sokoloff et al. 1998) and the resulting net polarization, from the combined random and mean field, can be either stronger or weaker than in the case of an isotropic random field depending on the sense of anisotropy relative to the orientation of the mean magnetic field. Note that the anisotropy of MHD turbulence resulting from the nature of the spectral energy cascade (Goldreich & Sridhar 1995; Lithwick et al. 2007; Galtier et al. 2000, and references therein) is important only at much smaller scales.

The case of M33 provides a suitable illustration of the refinements required if the anisotropy of the random magnetic field is significant. Tabatabaei et al. (2008, their Table 1) obtained integrated fractional polarization of about 0.1 at $\lambda 3.6$ cm. Using Eq. (3), this yields $\delta_b^2 \simeq 10$, whereas Eq. (4) leads to $\delta_b^2 \simeq 4$, consistent with their equipartition estimates $\sigma_b \simeq 6 \mu\text{G}$ and $B_0 \simeq 2.5 \mu\text{G}$. However, their analysis of Faraday rotation between $\lambda 3.6$, 6.2 and 20 cm suggests a weaker regular magnetic field, $B_0 \simeq 1 \mu\text{G}$, leading to $\delta_b^2 \simeq 40$ if $\sigma_b \simeq 6 \mu\text{G}$.

The latter estimate for B_0 is more reliable since the degree of polarization leads to an underestimated δ_b if magnetic field is anisotropic. Sokoloff et al. (1998, their Eq. (19)) have shown that the degree of polarization at short wavelengths in a partially ordered, anisotropic magnetic field is given by

$$p = p_0 \frac{1 + \delta_{by}^2(1 - \alpha_b^2)}{1 + \delta_{by}^2(1 + \alpha_b^2)},$$

where the (x, y) -plane is the plane of the sky with the y -axis aligned with the large-scale magnetic field, i.e., $B_y = B_0$ and $B_x = 0$; we further defined $\delta_{by}^2 = \sigma_{by}^2/B_0^2$ and likewise for δ_{bx} , and introduced $\alpha_b^2 = \sigma_{bx}^2/\sigma_{by}^2 (< 1)$ as a measure of the anisotropy of \mathbf{b}_{\perp} . This approximation is relevant to spiral galaxies where the mean magnetic field is predominantly azimuthal (nearly aligned with the y -axis of the local reference frame used here) and the anisotropy in the random magnetic field is produced by the rotational shear, $\sigma_{by} > \sigma_{bx}$. For $\delta_{by}^2 \gg 1$, this yields, for $p = 0.1$,

$$\alpha_b^2 \approx \frac{p_0 - p}{p_0 + p} \approx 0.8. \quad (5)$$

Thus, a rather weak anisotropy of the random magnetic field can produce $p \simeq 0.1$ and this allows us to reconcile the different estimates of δ_b obtained from the degree of polarization and Faraday rotation in M33.

The required anisotropy can readily be produced by the galactic differential rotation. Shearing of an initially isotropic random magnetic field by rotation (directed along the y -axis) leads, within one eddy turnover time, to an increase of its azimuthal component to

$$\sigma_{by} \simeq \sigma_{bx} \left(1 - r \frac{d\Omega}{dr} \frac{l}{v}\right),$$

where $\Omega(r)$ is the angular velocity of the galactic rotation (with the rotational velocity along the local y -direction and r the galactocentric radius) and l and v are the correlation length² and r.m.s.

² The correlation length l is also known as the integral scale and is defined as the integral of the variance-normalized autocorrelation function of a random variable. The typical linear size, or diameter, of a turbulent cell is $2l$.

speed of the interstellar turbulence, so that l/v is the lifetime of a turbulent eddy. This leads to

$$\alpha_b \simeq \left(1 - r \frac{d\Omega}{dr} \frac{l}{v}\right)^{-1} \simeq 1 - \frac{lV_0}{R_0v},$$

where the last equality is based on the estimate $r d\Omega/dr \simeq -V_0/R_0$, with $V_0 = 107 \text{ km s}^{-1}$ and $R_0 = 8 \text{ kpc}$ being the parameters of Brandt's approximation to the rotation curve of M33 (Rogstad et al. 1976). With $l = 0.1 \text{ kpc}$ and $v = 10 \text{ km s}^{-1}$ (values typical of spiral galaxies – e.g., Sect. VI.3 in Ruzmaikin et al. 1988), we obtain $\alpha_b^2 \simeq 0.8$, in perfect agreement with the degree of anisotropy required by Eq. (5) to explain the observations of Tabatabaei et al. (2008).

2.2 Summary

To conclude, a typical value of the relative strength of the random magnetic field in spiral galaxies is, at least,

$$\delta_b^2 \simeq 10. \quad (6)$$

This estimate refers to the correlation scale of interstellar turbulence, $l \simeq 50\text{--}100 \text{ pc}$. The correlation scale will be introduced in Section 4, but here we stress that this estimate refers to the larger scales in the turbulent spectrum. Higher values, $\delta_b^2 \simeq 40$ are perhaps more plausible, especially within spiral arms, but our results are not very sensitive to this difference (see Fig. 5 and Section 4). The estimate of δ_b in the Milky Way refers to the solar vicinity, i.e., to a region between major spiral arms where the degree of polarization is higher than within the arms and, correspondingly, δ_b is larger. Consistent with this, our analysis of the observed synchrotron fluctuations in Section 3 is for high Galactic latitudes and the outer parts of M33 where the influence of the spiral arms is not strong. Overall, $3 \lesssim \delta_b^2 \lesssim 40$ appears to be a representative range for spiral galaxies, excluding their central parts.

3 SYNCHROTRON INTENSITY FLUCTUATIONS DERIVED FROM OBSERVATIONS OF THE MILKY WAY AND M33

In this section we estimate the relative level of synchrotron intensity fluctuations from observations of the Milky Way and the spiral galaxy M33. An ideal data set for this analysis should: (i) resolve the fluctuations at their largest scale, (ii) only include emission from the ISM and not from discrete sources such as AGN and stars, (iii) not be dominated by structures that are large and bright due to their proximity, such as the North Polar Spur, (iv) be free of systematic trends such as arm-interarm variations or vertical stratification. The data should allow the ratio

$$\delta_I = \frac{\sigma_I}{I_0}, \quad (7)$$

where σ_I and I_0 are the standard deviation and the mean value of synchrotron intensity in a given region, to be calculated separately in arm and inter-arm regions or at low and high latitudes as I_0 differs between these regions. Regarding item (i) above, we note that a turbulent cell of 100 pc in size subtends the angle of about 6° at a distance of 1 kpc . Furthermore, most useful for our purposes are long wavelengths where the contribution of thermal radio emission is minimal. Unfortunately, ideal data satisfying all these criteria do not exist; we therefore use several radio maps, where each map possesses a few of the desirable properties listed above and collectively they have them all.

The Milky Way maps that we use contain isotropic emission from faint, unresolved extra-galactic sources and the cosmic microwave background. The contribution of the extragalactic sources to the brightness temperature of the total radio emission of the Milky Way is estimated by Lawson et al. (1987) as $T_e \simeq 50 \text{ K}(\nu/150 \text{ MHz})^{-2.75}$, which amounts to about 10^4 K and 3 K at the frequencies $\nu = 22 \text{ MHz}$ and 408 MHz , respectively. The 3 K temperature of the cosmic microwave background should also be taken into account at 408 MHz . For comparison, the respective total values of the radio brightness temperature near the north Galactic pole are about $3 \times 10^4 \text{ K}$ and 20 K at 22 MHz and 408 MHz , respectively. In our estimates of δ_I obtained below, we have not subtracted this contribution from I_0 . Thus, our estimates of δ_I are conservative, and more realistic values might be about 40% larger at both 22 MHz and 408 MHz . The observations of M33 use a zero level that is set at the edges of the observed area of the sky; since this zero level includes the CMB and unresolved extra-galactic sources δ_I is unaffected by these components.

3.1 The data

3.1.1 The 408 MHz all-sky survey

The survey of Haslam et al. (1982) covers the entire sky at a resolution of $51'$ (about 50 pc for a distance of 1 kpc) and with an estimated noise level of about 0.67 K . Synchrotron radiation is the dominant contribution to emission at the survey's wavelength of $\lambda 74 \text{ cm}$. The brightest structures in the map shown in Fig. 1a are the Galactic plane and several arcs due to nearby objects, especially the North Polar Spur.

We expect that results useful for our purposes arise at the angular scale of about 6° in all three Milky Way maps (i.e., the angular size of a turbulent cell at a 1 kpc distance), whereas larger scales reflect regular spatial variations of the radio intensity.

3.1.2 The 408 MHz all-sky survey, without discrete sources

La Porta et al. (2008) removed the strongest discrete sources from the data of Haslam et al. (1982) using a two-dimensional Gaussian filter. We compared the results obtained from the original 408 MHz survey with those from this map to show that the effect of point sources on our results is negligible.

3.1.3 The 22 MHz part-sky survey

Roger et al. (1999) produced a map, shown in Fig. 2a, of about 73% of the sky at $\lambda 13.6 \text{ m}$, between declinations -28° and $+80^\circ$ at a resolution of approximately $1^\circ \times 2^\circ$ and an estimated noise level of 5 kK . The emission is all synchrotron radiation, but H II regions in the Galactic plane absorb some background emission at this low frequency. However, we are most interested in regions away from the Galactic plane, so our conclusions are not affected by the absorption in the H II regions. The brightest point sources were removed by Roger et al. (1999) as they produced strong side-lobe contamination in the maps: this accounts for the four empty rectangles in Fig. 2a.

3.1.4 The 1.4 GHz map of M33

The nearby, moderately inclined, spiral galaxy M33 was observed at $\lambda 21 \text{ cm}$ by Tabatabaei et al. (2007a), using the VLA and Effelsberg telescopes, at a resolution of $51''$, or about 200 pc at the

distance to M33 of 840 kpc. The noise level is estimated to be 0.07 mJy/beam. The resolution is sufficient to resolve arm and inter-arm regions, but is at the top end of the expected scale of random fluctuations due to turbulence. The beam area includes a few (nominally, four) correlation cells of the synchrotron intensity fluctuations. The emission is a mixture of thermal and synchrotron radiation. The overall thermal fraction is estimated to be 18% but it is strongly enhanced in large H II regions and spiral arms (Tabatabaei et al. 2007b) whereas the synchrotron emission comes from the whole disc. The radio map used here is shown in Fig. 3a. The spiral pattern is notably weak in total synchrotron intensity, so the map appears almost featureless. This makes this galaxy especially well suited for our analysis since we are interested in quasi-homogeneous random fluctuations of the radio intensity. Nevertheless, systematic trends are noticeable in this map and we discuss their removal in Section 3.2.3.

3.2 Statistical parameters of the synchrotron intensity fluctuations

For the three Milky Way data sets of Sections 3.1.1–3.1.3, we calculated the mean I_0 and standard deviation σ_I of the synchrotron intensity I at each point in the map. In each case, the data were smoothed with a Gaussian of an angular width a , resulting in the local mean intensity at the scale a , which we denote I_{0a} :

$$I_{0a} = S_a^{-1} \iint I(l', b') \exp(-\theta^2/a^2) \cos b \, dl' \, db', \quad (8)$$

where integration extends over the data area, $\mathbf{r} = (l, b)$ is the position vector on the unit sky sphere, with l and b the Galactic longitude and latitude (confusion with the small-scale magnetic field, denoted here \mathbf{b} , should be avoided), $\theta = \arccos(\mathbf{r} \cdot \mathbf{r}')$ is the angular separation between \mathbf{r} and \mathbf{r}' ,

$$S_a(l, b) = \iint \exp(-\theta^2/a^2) \cos b \, dl' \, db',$$

is the averaging area, and the integration extends over the whole area of the sky available in a given survey. The standard deviation σ_{I_a} of radio intensity at a given position (l, b) at a given scale a is calculated as

$$\sigma_{I_a}^2(l, b) = \langle I^2 \rangle_a - \langle I \rangle_a^2,$$

where angular brackets denote spatial averaging as defined in Eq. (8).

In the case of M33, we selected nine areas which avoid the brightest H II regions and whose radio continuum emission is thus likely to be dominated by synchrotron radiation. Each area encompasses several beams and δ_I was calculated for each area, using the mean value and the standard deviation of I among all the pixels in the field obtained after removing regular trends (see Section 3.2.3).

3.2.1 The 408 MHz survey

To reduce the influence of the Galactic disc, where the structure in the radio maps is mainly due to systematic arm-interarm variations and localized radio sources such as supernova remnants, the original intensity data were truncated at 52 K (1% of the maximum and 167% of the r.m.s. value of I): this blanking only affects emission at Galactic latitudes $|b| < 20^\circ$. The resulting sky distribution of the relative radio intensity fluctuations σ_{I_a}/I_{0a} is shown in Fig. 1 for a selection of averaging scales, $a = 30^\circ$, 15° and 7° (a corresponds to the radius rather than the diameter of the region).

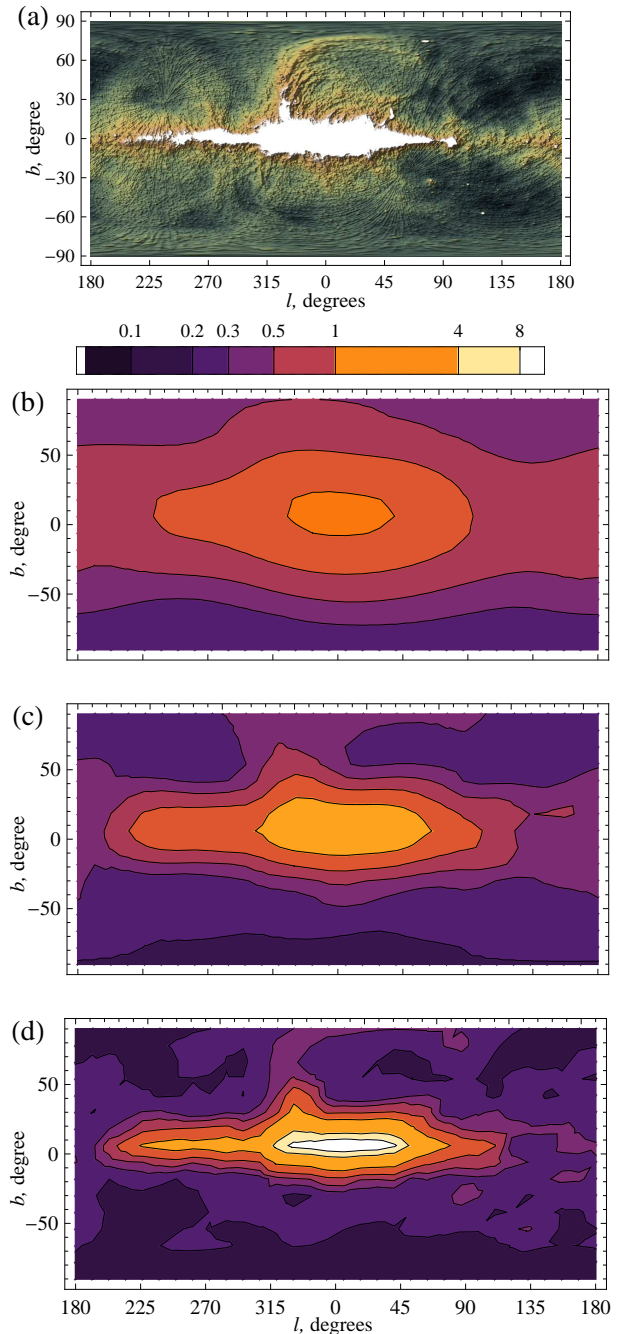


Figure 1. (a): The 408 MHz all-sky map of the total synchrotron intensity (Haslam et al. 1982), with the Galactic disc area ($I > 52$ K) blanked out. The lower panels show the magnitude of the relative fluctuations of the synchrotron intensity, $\delta_I = \sigma_I/I_0$, at various scales, with the colour bar shown between Panels (a) and (b): (b) $a = 30^\circ$, (c) $a = 15^\circ$ and (d) $a = 7^\circ$. The latter scale is about the angular size of a turbulent cell ($2l_\varepsilon = 100$ pc) seen at a distance 1 kpc.

While panels (b) and (c) in Fig. 1 reflect mainly systematic trends in radio intensity, we expect that panel (d) is dominated by the turbulent fluctuations. In particular, the $a = 7^\circ$ map shows a much weaker variation with Galactic latitude than those at larger scales, for $|b| \gtrsim 30^\circ$. We note that the corre-

Table 1. Relative radio intensity fluctuations σ_I/I_0 in M33 with systematic trends of various orders subtracted. The first column gives the field number as specified in Fig. 3, and the next three columns show the relative fluctuations of radio intensity, with $\sigma_I^{(m)}$ the standard deviation of I within a given field, obtained with a trend of order m subtracted (the mean value of the trend vanishes across each field): $m = 0$ corresponds to the original data, $m = 1$, to a linear trend, and $m = 2$, to a quadratic trend in the angular coordinates. The last column shows the mean value of the radio intensity in each field.

Field No.	$\sigma_I^{(0)}/I_0$	$\sigma_I^{(1)}/I_0$	$\sigma_I^{(2)}/I_0$	I_0 [$\mu\text{Jy}/\text{beam}$]
1	0.30	0.18	0.14	677
2	0.34	0.22	0.19	545
3	0.31	0.15	0.11	609
4	0.28	0.18	0.17	606
5	0.38	0.17	0.13	672
6	0.35	0.15	0.12	795
7	0.30	0.16	0.14	565
8	0.32	0.07	0.07	902
9	0.38	0.14	0.11	810
Mean	0.33	0.16	0.13	687

lation scale of the synchrotron intensity fluctuations obtained by Dagkesamanskii & Shutenkov (1987) is 8° .

At $|b| \gtrsim 20^\circ$, the maximum pathlength through the synchrotron layer is about $h_\epsilon/\sin b \simeq 6$ kpc, where the synchrotron scale height $h_\epsilon \simeq 1.8$ kpc (Beuermann et al. 1985). With an angular resolution of about 1° the linear beamwidth is about 100 pc at most. Give that the correlation length is about $l_c \simeq 50$ pc (see Section 6.3) the beam encompasses one synchrotron cell at most.

Contours outside the Galactic disc in Fig. 1d, $|b| \gtrsim 30^\circ$ give

$$\delta_I = 0.1\text{--}0.2. \quad (9)$$

Results obtained from the 408 MHz map with point sources subtracted differ insignificantly from those obtained using the original map.

3.2.2 The 22 MHz partial sky survey

Contours of the relative intensity fluctuations obtained from the 22 MHz map are shown in Fig. 2. As in Fig. 1, averaging over scales $a = 30^\circ$ and 15° reveals the large-scale structure clearly visible in the original data. However, results at $a = 7^\circ$ show much less of such structure, and the statistically homogeneous part of the sky in this panel includes the same contours of 0.1 and 0.2 as in Fig. 1, with the value of 0.3 confined to the bright ridges seen in Fig. 2a. Thus, the 22 MHz data are in a good agreement with the values for δ_I obtained from the 408 MHz data. This suggests a weak frequency dependence of the relative synchrotron intensity fluctuations δ_I .

3.2.3 M33

Our analysis for the Milky Way has a potential difficulty that long lines of sight might make it impossible to separate the contributions to σ_I from small-scale (random) and large-scale (systematic) variations of the synchrotron emissivity. Therefore, we consider also the nearby galaxy M33 seen nearly face-on (inclination 56°). To avoid excessive contribution from large-scale variations due to the spiral pattern and the radial gradient in I , we selected areas free of strong

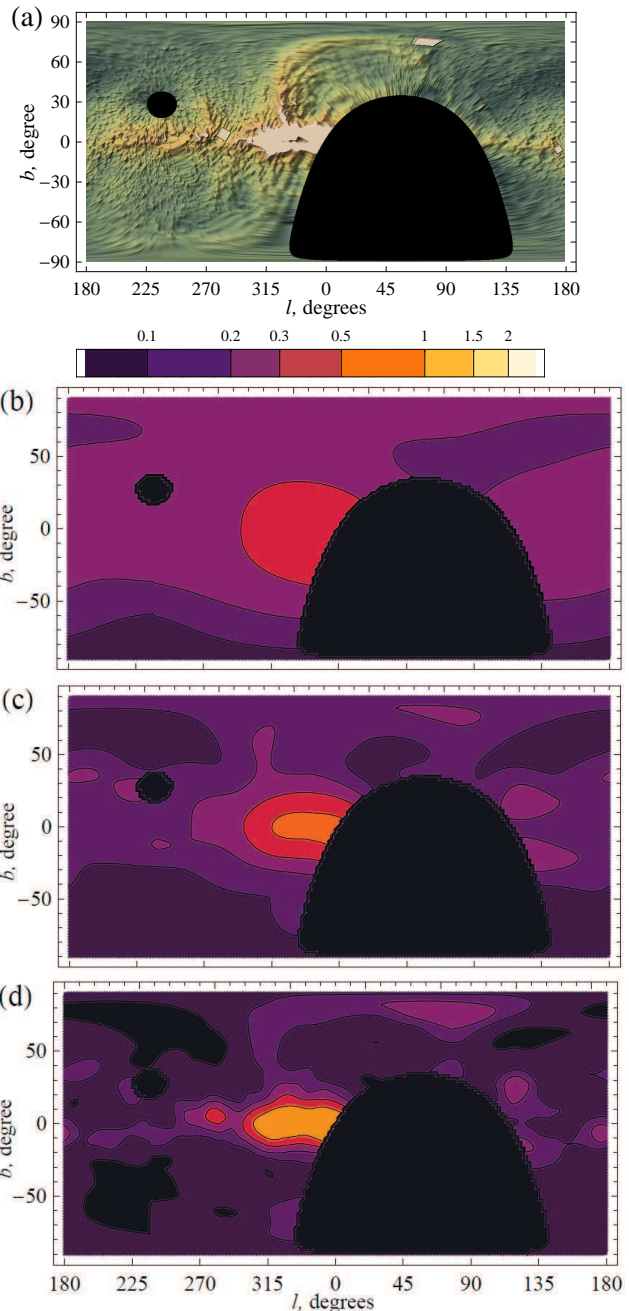


Figure 2. As in Fig. 1 but for the 22 MHz survey (Roger et al. 1999) with the Galactic disc area ($I > 10^5$ K) blanked out.

star formation in the outer regions of the galaxy disc in Fig. 3. The areas of the rectangular fields chosen range from 1.9×1.2 kpc² to 1.9×4.7 kpc².

The fields are big enough to make gradients in the mean quantities significant; in particular, the non-thermal disc of M33 has a strong radial gradient in radio intensity (Tabatabaei et al. 2007b), so we subtract regular trends from the values of I . We fitted first- or second-order polynomials to $I(l, b)$ in l and b in each field and calculated δ_I after subtracting the trends with vanishing mean value from the original data. Results are shown in Table 1, with $\sigma_I^{(m)}$ denoting the standard deviation of the radio intensity obtained upon

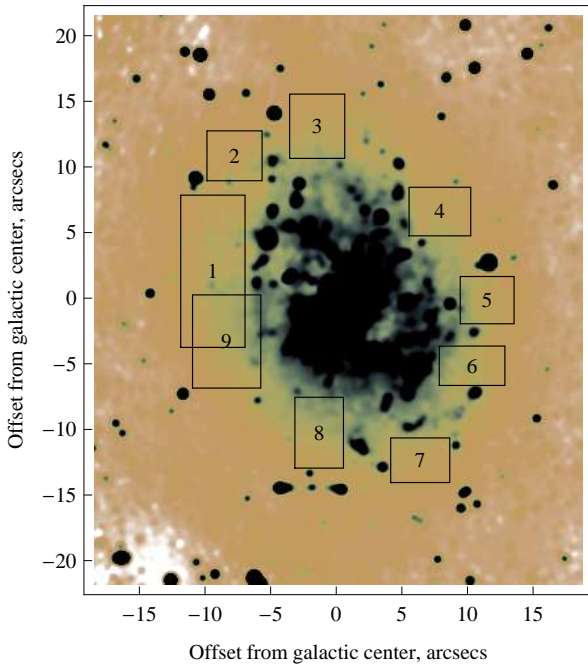


Figure 3. The 1.4 GHz radio map of M33 (Tabatabaei et al. 2007a), with the rectangular fields used in our analysis shown. For orientation, we note that the size of Field 3 is $7' \times 7'$ equivalent to $1.6 \times 1.9 \text{ kpc}^2$.

the subtraction of a polynomial of order m in the angular coordinates. The mean value of synchrotron intensity I_0 was calculated for each field.

We note that $\sigma_I^{(0)}$ (the standard deviation of I in the original data) is noticeably larger than $\sigma_I^{(1)}$ and $\sigma_I^{(2)}$. Thus, the large-scale trends contribute significantly to the intensity variations. On the other hand, $\sigma_I^{(1)}$ and $\sigma_I^{(2)}$ have rather similar magnitudes of about 0.15 (and $\sigma_I^{(1)} > \sigma_I^{(2)}$ as expected), so that they can be adopted as an estimate of σ_I corrected for the large-scale trends. We use the value of $\sigma_I^{(2)}/I_0$ averaged over the nine fields explored as the best estimate for δ_I .

However, $W \approx 100 \text{ pc}$ (half-width at half maximum of the Gaussian beam) in the observations of M33 used here. Assuming the synchrotron correlation length $l_\epsilon = 50 \text{ pc}$ the beam area encompasses $N_W \approx 4$ correlation cells. Therefore, to make the M33 results (especially δ_I) comparable to those of the Milky Way, we have to reduce them to a common pathlength and number of synchrotron correlation cells within the beam. We recall that the beams at 408 MHz and 22 MHz only cover at most one synchrotron cell (see Section 3.2.1), so we have $N_W = 1$ in the Milky Way. For the small value of N_W in the high-resolution observations of M33, the dependence of δ_I differs significantly from its asymptotic form $\delta_I \propto N_W^{-1/2}$. Figure 4 shows the dependence of δ_I on N_W obtained for a model synchrotron-emitting system described in detail in Section 5: δ_I only weakly depends on N_W for small N_W . Reduced to a single line of sight, the synchrotron intensity fluctuations in M33 then correspond to $\delta_I = 0.13/0.7 = 0.2$ if the synchrotron correlation length is $l_\epsilon = 50 \text{ pc}$ (i.e., $N_W = 4$). We also recall that the typical pathlength through the disc of M33 is about twice that through the Milky Way (where the observer is located not far from the midplane), and we adopt $L \approx 1 \text{ kpc}/\cos(i) \approx 2 \text{ kpc}$ (Tabatabaei et al. 2008) for this galaxy. Then the value of δ_I in M33, reduced to a standard value of $L = 1 \text{ kpc}$ for compatibil-

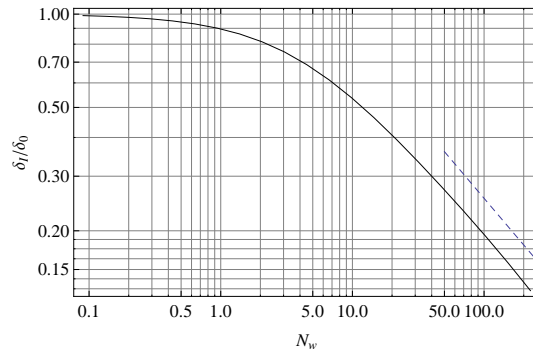


Figure 4. The relative fluctuations in synchrotron intensity δ_I as a function of N_W , the number of synchrotron correlation cells across the beam area, with δ_I normalized by δ_0 , the relative fluctuations obtained along a single line of sight, i.e., for $N_W \rightarrow 0$. The asymptotic dependence $\delta_I = 2\delta_0 N_W^{-1/2}$ (dashed line) emerges only for $N_W \gtrsim 20$ –30. The calculation assumed a Gaussian beam, with the full width at half-maximum (FWHM) taken for the beam diameter.

ity with the Milky Way data, is further $\sqrt{2}$ times larger:

$$\delta_I \simeq 0.3.$$

3.3 Comparison with earlier results and summary

To date, analysis of synchrotron observations of the Milky Way has focused primarily on the spectrum of the fluctuations while their magnitude has attracted surprisingly little attention. Mills & Slee (1957) observed fluctuations of the Galactic radio background near the Galactic south pole at $\lambda = 3.5 \text{ m}$, with the resolution of 50° , to obtain $\sigma_I = 3.3 \times 10^{-26} \text{ W m}^{-2} \text{ Hz}^{-1}$ per beam, which corresponds to $\delta_I = 0.12$ (see also Getmantsev 1959).

Dagkesamanskii & Shutenkov (1987) used observations at 102.5 MHz ($\lambda 2.92 \text{ m}$) near the North Galactic Pole, where the Galactic radio emission is minimum, to determine the synchrotron autocorrelation function and its anisotropy arising from the large-scale magnetic field. They obtain $\delta_I \approx 0.07$ but note that this estimate should be doubled if the isotropic extragalactic background (half the total flux) is to be subtracted, to yield $\delta_I \simeq 0.14$. Banday et al. (1991a) argue that only 17% of the total flux is of extragalactic origin, and then $\delta_I \simeq 0.08$ at 102.5 MHz.

The autocorrelation function of the brightness temperature fluctuations of the Galactic radio background was determined also by Banday et al. (1991a,b) who used observations at 408 and 1420 MHz, smoothed to a resolution of about FWHM = 5° . They observed a ‘quiet’ region with reduced fluctuations, $30^\circ < \text{DEC} < 50^\circ$, $180^\circ < \text{RA} < 250^\circ$, identified by Bridle (1967) as an inter-arm region, since they were interested in the cosmic microwave background fluctuations. For the Galactic synchrotron radiation, which dominates at these frequencies, they obtain $\delta_I \approx 0.05$ at 408 MHz and 0.08 at 1420 MHz.

These estimates are somewhat lower than those obtained above. The value of δ_I obtained by Banday et al. can be lower due to their selection of a region with weaker synchrotron intensity fluctuations.

The relative fluctuations in radio intensity are remarkably similar in all the Milky Way maps and in all fields in M33 considered,

with

$$\delta_I \approx 0.1\text{--}0.3,$$

when reduced to the common pathlength $L = 1$ kpc (see Section 6.2 for further discussion). The lower values are more plausible. We believe that these estimates are not significantly affected by either large-scale trends in the radio intensity or by discrete radio sources or by thermal emission. Even if these effects still contribute to our estimate, it provides an *upper* limit on the fluctuations in synchrotron intensity arising in the interstellar medium of the Milky Way and M33.

4 STATISTICAL ANALYSIS OF SYNCHROTRON INTENSITY FLUCTUATIONS

In order to interpret the results of our analysis of observations in Section 3, we use a model of partially ordered, random distributions of magnetic fields and cosmic rays, assuming various degrees of correlation (or anticorrelation) between them. We calculate the relative magnitude of synchrotron intensity fluctuations δ_I analytically and numerically and compare the results with the observational constraints described above in order to establish to estimate the degree of correlation or anticorrelation compatible with observations.

In this Section, first we relate fluctuations in synchrotron intensity to the underlying synchrotron emissivity, then we describe a model for defining distributions of magnetic field and cosmic rays with controlled cross-correlation. These magnetic field and cosmic ray distributions allow us to calculate the model synchrotron emissivity, using results derived in Appendix A, and hence the model synchrotron intensity.

4.1 Relative fluctuations of synchrotron intensity

Here we estimate the synchrotron intensity $I_0 = \langle I \rangle_S$ averaged over an area S in the plane of the sky and the corresponding standard deviation, $\sigma_I = (\langle I^2 \rangle_S - \langle I \rangle_S^2)^{1/2}$, as a function of the synchrotron emissivity. Angular brackets are used to denote various spatial averages (over an area S , volume V or path length L , as indicated by the corresponding subscript), whereas overbar is used for statistical (ensemble) averages. The former arise naturally from observations and numerical models, whilst analytical calculations usually provide the latter. We assume that the two types of averaging procedure lead to identical results (unlike Gent et al. 2013), although we distinguish them formally for the sake of clarity.

Assuming that the synchrotron spectral index is equal to -1 (this simplifies analytical calculations significantly, without noticeable effect on the results – see Section 8 below), the intensity of synchrotron emission at a given position in the sky is given by

$$I = \int_L \varepsilon \, ds \propto \int_L n_{\text{cr}} B_{\perp}^2 \, ds, \quad (10)$$

where ε is the synchrotron emissivity, n_{cr} is the number density of cosmic ray electrons, B_{\perp} is magnetic field in the plane of the sky and integration is carried along the line of sight s over the path length L .

In a random magnetic field and cosmic-ray distribution, the synchrotron emissivity I is also a random variable. We can rewrite Eq. (10) in terms of the path-length average as

$$I = L \langle \varepsilon \rangle_L, \quad (11)$$

where $\langle \varepsilon \rangle_L = L^{-1} \int_L \varepsilon \, ds$ is the average synchrotron emissivity along the path length. We neglect a dimensional factor in Eq. (11) and other similar equations; it is unimportant as we always consider relative fluctuations where it cancels. The average synchrotron intensity from the area S in the sky plane is then related to the synchrotron emissivity averaged over the volume of a depth L (the extent of the radio source along the line of sight) and cross-section S :

$$I_0 = \langle I \rangle_S = L \langle \varepsilon \rangle_V = 2N l_{\varepsilon} \bar{\varepsilon}, \quad (12)$$

where l_{ε} is the correlation length of the synchrotron emissivity, $N = L/(2l_{\varepsilon}) (\gg 1)$ is the number of correlation cells of ε along the path length L , and the volume average has been identified with the statistical average to obtain the last equality,

$$\langle \varepsilon \rangle_V = \bar{\varepsilon}. \quad (13)$$

If S is sufficiently large, such an identification applies to the area average as well, but the linear resolution of observations often approaches the size of a turbulent cell in the source; in this case, Eq. (13) is more appropriate.

Fluctuations in I arise from variations of both ε and L between different lines of sight. Neglecting the latter, the standard deviation of I follows as

$$\sigma_I = N^{-1/2} L \sigma_{\varepsilon} = \sigma_{\varepsilon} (2l_{\varepsilon} L)^{1/2}, \quad N \gg 1; \quad (14)$$

this quantity characterizes the scatter in the synchrotron intensity at different positions across the radio source separated by more than l_{ε} to make them statistically independent.

4.2 Cosmic ray distribution partially correlated with magnetic field

In this section we introduce a distribution of cosmic rays which has a prescribed cross-correlation coefficient with a given magnetic energy density. Magnetic field is represented as the sum of the mean and random parts, \mathbf{B}_0 and \mathbf{b} , respectively:

$$\mathbf{B} = \mathbf{B}_0 + \mathbf{b},$$

with $\bar{\mathbf{b}} = 0$, $\bar{\mathbf{B}} = \mathbf{B}_0$ and $\overline{B^2} = B_{0\perp}^2 + B_{0\parallel}^2 + \sigma_b^2$, where $B_{0\perp}$ and $B_{0\parallel}$ are the mean field components in the plane of the sky and parallel to the line of sight, respectively. Each Cartesian vectorial component of the random magnetic field \mathbf{b} is assumed to be a Gaussian random variable with zero mean value, $\bar{b}_i = 0$, and to avoid unnecessary complicated calculations, the random magnetic field is assumed to be isotropic,

$$\overline{b_i^2} = \frac{1}{3} \overline{b^2} = \frac{1}{3} \sigma_b^2, \quad (15)$$

where $i = x, y, z$ and overbar denotes ensemble averaging.

The number density of cosmic-ray electrons is similarly represented as the sum of a mean $n_0 \equiv \bar{n}_{\text{cr}}$ (slowly varying in space) and random n' parts,

$$n_{\text{cr}} = n_0 + n'. \quad (16)$$

The cross-correlation coefficient c of n_{cr} and B^2 is defined as

$$c(B^2, n_{\text{cr}}) = \frac{\overline{n_{\text{cr}} B^2} - \bar{n}_{\text{cr}} \overline{B^2}}{\sigma_n \sigma_{B^2}}. \quad (17)$$

To implement local equipartition between cosmic rays and magnetic field, which corresponds to $c = 1$, we use a distribution of cosmic rays identical to that of the random part of the magnetic

energy density, $n' = \alpha(B^2 - \overline{B^2})$, where α is a coefficient that allows us to control independently the magnitude of the fluctuations in n_{cr} .

To obtain partially correlated distributions of n_{cr} and B^2 , we introduce an auxiliary positive-definite, scalar random field F , uncorrelated with the magnetic energy density:

$$c(B^2, F) = 0. \quad (18)$$

Our specific choice of B and F is discussed below.

Now, we represent the random part of the cosmic-ray number density as

$$n' = \alpha(B^2 - \overline{B^2}) + \beta(F - \overline{F}), \quad (19)$$

where the coefficients α and β are chosen to obtain

$$c(B^2, n_{\text{cr}}) = C, \quad (20)$$

with C the desired value of the cross-correlation coefficient. The first term in Eq. (19) is responsible for the part of the cosmic-ray distribution fully correlated with magnetic field energy density, whereas the second term reduces the cross-correlation to the desired level. In particular, Eq. (19) ensures that $c(B^2, n_{\text{cr}}) = 1$ for $\alpha = 1, \beta = 0$ (perfect correlation), and $c(B^2, n_{\text{cr}}) = 0$ for $\alpha = 0$ (uncorrelated distributions).

Let us find α and β from Eq. (20). It follows from Eqs (16) and (19) that

$$\overline{n_{\text{cr}} B^2} = \alpha \sigma_{B^2}^2 + n_0 \overline{B^2}$$

given that Eq. (18) implies

$$\overline{B^2 F} = \overline{B^2} \overline{F}.$$

For any uncorrelated random variables X and Y , the variance of their sum $Z = X + Y$ is given by $\sigma_Z^2 = \sigma_X^2 + \sigma_Y^2$. Hence, Eq. (19) implies

$$\sigma_n^2 = \alpha^2 \sigma_{B^2}^2 + \beta^2 \sigma_F^2. \quad (21)$$

Then Eq. (20) yields

$$\frac{\alpha}{\sqrt{\alpha^2 \sigma_{B^2}^2 + \beta^2 \sigma_F^2}} = C, \quad (22)$$

where $\sigma_{B^2} = \overline{B^4} - (\overline{B^2})^2$ and $\sigma_F^2 = \overline{F^2} - \overline{F}^2$. Using Eq. (21) to eliminate β in Eq. (22), we obtain

$$\alpha = \frac{\sigma_n}{\sigma_{B^2}} C \quad \text{and} \quad \beta = \frac{\sigma_n}{\sigma_F} \sqrt{1 - C^2}.$$

Equation (19) then reduces to

$$n_{\text{cr}} = n_0 + \sigma_n \left(C \frac{B^2 - \overline{B^2}}{\sigma_{B^2}} + \sqrt{1 - C^2} \frac{F - \overline{F}}{\sigma_F} \right), \quad (23)$$

where the standard deviation of the cosmic-ray number density σ_n is an independent parameter that we are free to vary.

Our specific model of magnetic field is described in Section 5. However, for the analytical calculations of δ_I presented in Section 4.3, it is sufficient to know B_0 and σ_B . There is no need to specify F in any more detail as long as F and B^2 (more precisely, B_{\perp}^2) are uncorrelated. The more detailed model of Section 5 is only required for numerical calculations presented below to verify and refine the analytical results.

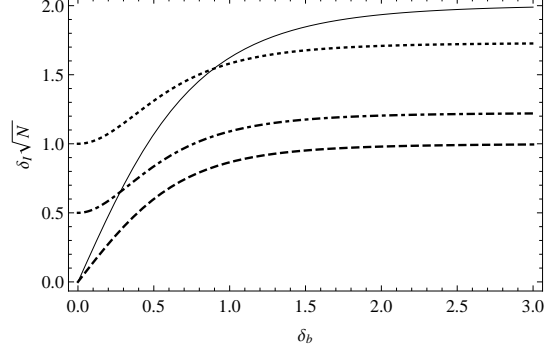


Figure 5. The relative fluctuations in synchrotron intensity δ_I versus the relative magnitude of magnetic field fluctuations δ_b obtained analytically in four special cases. Solid line, Eq. (24), is for complete correlation of cosmic rays and magnetic fields, $C = 1$; dashed line is from Eq. (26), i.e., $n_{\text{cr}} = \text{const}$; dotted and dash-dotted lines were obtained from Eq. (25) for uncorrelated fluctuations in cosmic rays and magnetic field, $C = 0$, with $\delta_n = 1$ and $\delta_n = 0.5$, respectively. We note that the curves rapidly approach the horizontal asymptote, so that the approximation $\delta_b \rightarrow \infty$ is reasonably accurate for $\delta_b > 1.5\text{--}2$ as typically found in spiral galaxies.

4.3 Synchrotron intensity fluctuations with partially correlated n_{cr} and B^2

Details of the calculations of $\overline{\varepsilon}$ and σ_{ε} , and then, of the mean value and standard deviation of the synchrotron intensity using Eqs (12) and (14) together with Eq. (23) can be found in Appendix A, with I_0 given by Eq. (A2) and σ_I by Eq. (A3). Here we consider the key special cases.

The model developed here allows us to express δ_I in terms of the following dimensionless parameters: the number of correlation cells along the line of sight N (assuming perfect angular resolution; a finite beam size can be allowed for using additional averaging across the beam as in the end of Section 3.2.3), the cross-correlation coefficient between cosmic rays and magnetic field C , the relative magnitude of the magnetic field fluctuations δ_b , and the relative magnitude of fluctuations in cosmic ray number density,

$$\delta_n = \frac{\sigma_n}{n_0}.$$

In the case of detailed (local, or pointwise) equipartition between cosmic rays and magnetic fields, $n_{\text{cr}} \propto B^2$, $C = 1$ and $\delta_n = \sigma_{B^2}/B^2$ (Eq. (A4)) so the relative fluctuations in the synchrotron intensity follow as

$$\delta_I = \frac{\sigma_I}{I_0} = \frac{\delta_b (54 + 295\delta_b^2 + 404\delta_b^4 + 101\delta_b^6)^{1/2}}{N^{1/2} (3 + 10\delta_b^2 + 5\delta_b^4)}. \quad (24)$$

We recall that $\delta_b = \sigma_b/B_0$ and note that all such analytical results are valid only for $N \gg 1$. As δ_b increases, δ_I rapidly approaches the asymptotic value independent of δ_b (see Fig. 5):

$$\delta_I \simeq 2N^{-1/2} \quad \text{for} \quad \delta_b^2 \gg 1.$$

It is useful to note similar expressions for δ_I obtained under different assumptions about the correlation between cosmic rays and magnetic field. If cosmic ray fluctuations are uncorrelated with those in magnetic field, Eqs. (A2) and (A3) yield for $C = 0$

$$\delta_I = \frac{[\delta_n^2 + \delta_b^2(2 + \delta_b^2)(1 + 2\delta_n^2)]^{1/2}}{N^{1/2} (1 + \delta_b^2)}. \quad (25)$$

In particular, for $\delta_n \rightarrow 0$ we obtain an asymptotic form for a ho-

mogeneous distribution of cosmic rays:

$$\delta_I = \frac{\delta_b(2 + \delta_b^2)^{1/2}}{N^{1/2}(1 + \delta_b^2)}. \quad (26)$$

Thus, $\delta_I \simeq N^{-1/2}$ for $\delta_b^2 \gg 1$ and $n_{\text{cr}} = \text{const}$. Figure 5 shows the dependence of δ_I on δ_b from Eqs (24), (25) and (26).

It is convenient to summarize these results by providing the corresponding values of a quantity independent of the number of correlation cells along the path length, $N^{1/2}\delta_I$, as obtained from Eqs (24), (25) and (26) for $\delta_b \gg 1$, which is applicable to $\delta_b \simeq 3$ (Fig. 5). The relative magnitude of synchrotron intensity fluctuations expected under detailed equipartition follows from Eq. (24) as

$$N^{1/2}\delta_I \approx 2.0 \quad (\text{local equipartition}). \quad (27)$$

Equation (25) yields, for $\delta_n = 0.5$,

$$N^{1/2}\delta_I \approx 1.2 \quad (\text{uncorrelated fluctuations}),$$

and Eq. (26) leads to

$$N^{1/2}\delta_I \approx 1.0 \quad (n_{\text{cr}} = \text{const}).$$

As might be expected, detailed equipartition between cosmic rays and magnetic fields leads to the strongest synchrotron intensity fluctuations for a given δ_b and N . For illustration, with the correlation length of the synchrotron intensity fluctuations $l_\varepsilon = 50$ pc and the path length $L = 1$ kpc, we obtain $N = L/2l_\varepsilon \simeq 10$ for a beam narrower than the size of the correlation cell. We note that the dependence of $\sqrt{N}\delta_I$ on δ_b is quite weak as long as $\delta_b^2 \gtrsim 3$ which is usually the case for spiral galaxies (see Section 2). The difference in the level of synchrotron fluctuations in these limiting cases is strong enough to be observable under certain conditions clarified in Section 6.

5 A MODEL OF A PARTIALLY ORDERED MAGNETIC FIELD

To verify, strengthen and refine the analytical calculations presented above, we implement numerically the model of magnetic field and cosmic rays described in Section 4.2. For this purpose, we introduce in this section a multi-scale magnetic field with prescribed spectral properties and the corresponding cosmic-ray distribution using Eq. (23). The phases and directions of individual modes in the magnetic field spectrum can be chosen at random without affecting the magnetic field correlation scale, the value of δ_B and the energy spectrum. We use this freedom to generate a large number of statistically independent realizations of the magnetic field and cosmic-ray distributions to compute the resulting values of δ_I and compare them with the analytical results.

To prescribe a quasi-random magnetic field \mathbf{b} with vanishing mean value in a periodic box, we use a Fourier expansion in modes with randomly chosen directions of wave vectors \mathbf{k} , but with amplitudes adjusted to reproduce any desired energy spectrum:

$$\mathbf{b}(\mathbf{x}) = \frac{1}{(2\pi)^{3/2}} \int \hat{\mathbf{b}}(\mathbf{k}) e^{i\mathbf{k}\cdot\mathbf{x}} d^3\mathbf{k}, \quad (28)$$

where $\hat{\mathbf{b}}$ is the Fourier transform of \mathbf{b} ; the physical field is represented by the real part of this complex vector. The corresponding magnetic energy spectrum is given by

$$M(k) = \int_{|\mathbf{k}'|=k} |\hat{\mathbf{b}}(\mathbf{k}')|^2 d^3\mathbf{k}', \quad (29)$$

where the integral is taken over the spherical surface of a radius k in k -space. In the isotropic case, $M(k) = 4\pi k^2 |\hat{\mathbf{b}}(k)|^2$. In order to ensure periodicity within a computational box of size L , as required for the discrete Fourier transformation, the components of the wave vectors are restricted to be integer multiples of $2\pi/L$.

A solenoidal vector field \mathbf{b} , i.e., that having $\mathbf{k} \cdot \hat{\mathbf{b}}(\mathbf{k}) = 0$, is specified by

$$\hat{\mathbf{b}}(\mathbf{k}) = \frac{\mathbf{k} \times \mathbf{X}}{|\mathbf{k} \times \mathbf{X}|} k^{-1} \sqrt{M(k)},$$

where \mathbf{X} is a complex vector chosen at random, to ensure that the Fourier modes have random phases. We consider a magnetic energy spectrum represented by two power-law ranges,

$$M(k) = M_0 \begin{cases} (k/k_0)^{s_0} & \text{for } k < k_0, \\ (k/k_0)^{-s_1} & \text{for } k \geq k_0, \end{cases} \quad (30)$$

with $s_0 > 0$ and $s_1 > 0$, where k_0 is the energy-range wavenumber. We use $s_1 = 5/3$ as in Kolmogorov's spectrum and $s_0 = 2$ (see Christensson et al. 2001). The standard deviation of the magnetic field is given by

$$\sigma_b^2 = \int_0^\infty M(k) dk = M_0 k_0 \frac{s_0 + s_1}{(s_0 + 1)(s_1 - 1)} \quad (31)$$

for $s_1 > 1$. The correlation length l_b of the resulting magnetic field (analogous to the radius of a correlation cell) differs from its dominant half-wavelength $\frac{1}{2}\lambda_0 = \pi/k_0$ for any finite values of s_0 and s_1 (Monin & Yaglom 1975):

$$\begin{aligned} l_b &= \frac{\pi}{2} \frac{\int_0^\infty k^{-1} M(k) dk}{\int_0^\infty M(k) dk} = \frac{\pi}{2k_0} \left(1 + \frac{1}{s_0}\right) \left(1 - \frac{1}{s_1}\right) \\ &= \frac{3\pi}{10k_0}, \end{aligned} \quad (32)$$

where the last equality follows for $s_0 = 2$ and $s_1 = 5/3$. For the Milky Way, suitable values are $l_b = 50$ pc and $\sigma_b \simeq 5\text{--}10 \mu\text{G}$ (see Sections 2 and 8).

The resulting solenoidal vector field is then added to a uniform component \mathbf{B}_0 to produce a partially ordered magnetic field with controlled fluctuation level δ_b and energy spectrum $M(k)$. This approach has been used to generate synthetic polarization maps of the turbulent ISM by Stepanov et al. (2008); Volegova & Stepanov (2010); Arshakian et al. (2011); Moss et al. (2012). Similar constructions were used by Giacalone & Jokipii (1999) and Casse et al. (2002) in their modelling of cosmic ray propagation in random magnetic fields, by Malik & Vassilicos (1999) for modelling turbulent flows, and by Wilkin et al. (2007) to study dynamo action in chaotic flows.

We will now verify, by direct calculation, that $C(B^2, n_{\text{cr}}) \approx C$. The reason for the approximate equality is first explained.

A shortcoming of the analytical cosmic ray model defined by Eqs. (16) and (19) is that n_{cr} can be negative at some positions (especially when $C < 0$ and hence $\alpha < 0$) because, at some positions and in some realizations, B^2 can be arbitrarily large (as a Gaussian random variable squared). This deficiency could be corrected by selecting a more realistic probability distribution for \mathbf{b} (e.g., a truncated Gaussian) but we do not feel that this would lead to any additional insight. In the numerical calculations described below, we truncate the negative values of n_{cr} by replacing them with zero. This, however, makes it impossible to achieve exact anticorrelation between cosmic rays and magnetic fields, so that $C(B^2, n_{\text{cr}}) > -1$.

In analytical calculations, we restrict ourselves to the cases with $\delta_n < 1$ to reduce the extent of the problem (even if not to

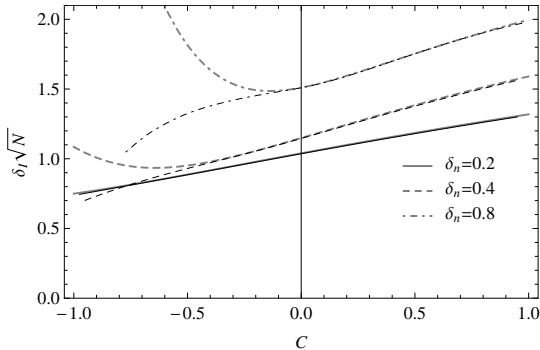


Figure 6. The relative fluctuations in synchrotron intensity δ_I as obtained from analytical formulae Eqs. (A2 and A3) (thicker curves) and from numerical calculations with the condition $n_{\text{cr}} > 0$ enforced (the corresponding thinner curves), for: $\delta_n = 0.2$ (solid), $\delta_n = 0.4$ (dashed) and $\delta_n = 0.8$ (dash-dotted). The analytic formulae become inapplicable for $C < 0$ and $\delta_n \simeq 1$ (see the text). The magnetic field is purely random, $B_0 = 0$ and $N = 10$.

resolve it completely). For example, Eqs. (A2) and (A3) yield for $\delta_b \rightarrow \infty$ (note that δ_I is constant with respect to δ_b for $\delta_b \gtrsim 3$ (Fig. 5))

$$\delta_I = \frac{[9 + 6\delta_n (11C^2\delta_n + 3\sqrt{6}C + 3\delta_n)]^{1/2}}{N^{1/2}(\sqrt{6}C\delta_n + 3)}. \quad (33)$$

This dependence of δ_I on the cross-correlation coefficient C is shown with thicker curves in Fig. 6 for various values of the relative fluctuations in cosmic rays, δ_n . Thinner curves show similar results obtained from a numerical calculation where $n_{\text{cr}} > 0$ is enforced. It is clear from Fig. 6 that these analytical results are accurate for $C > 0$.

However, for $C < 0$, analytic results are useful only if the fluctuations in the cosmic ray number density are relatively weak: $C \gtrsim -0.1$ for $\delta_n < 0.8$, $C \gtrsim -0.5$ for $\delta_n < 0.4$, and almost any value of C for $\delta_n < 0.2$. We only use these analytical results for illustrative purposes, whereas all our conclusions are based on numerical results where $n_{\text{cr}} > 0$ at all positions. Nevertheless, the analytic results presented here and in Appendix A, however unwieldy, are simpler to use than constructing a numerical model and are accurate for δ_n small enough (say, $\delta_n \lesssim 0.4$) and C large enough (say, $C \gtrsim -0.5$) — see Fig. 6.

6 RESULTS

6.1 Synthetic radio maps

Each component of the magnetic field described by Eq. (28) is the sum of a large number of independent contributions from different wave numbers. By virtue of the central limit theorem, each component of the resulting magnetic field is well approximated by a Gaussian random variable. Then the mean synchrotron intensity and its standard deviation over N correlation cells can be expressed, using Eq. (10), in terms of B_0 , σ_b , δ_n and C . Explicit analytic expressions for I_0 and σ_I can be found in Appendix A, and we illustrate these results in Fig. 6. As might be expected, the relative level of the synchrotron intensity fluctuations increases with the cross-correlation coefficient between B^2 and n_{cr} .

Since analytical results are of limited relevance for $C < 0$, we performed numerical calculations of the synchrotron intensity where the cosmic-ray number density is truncated to be non-

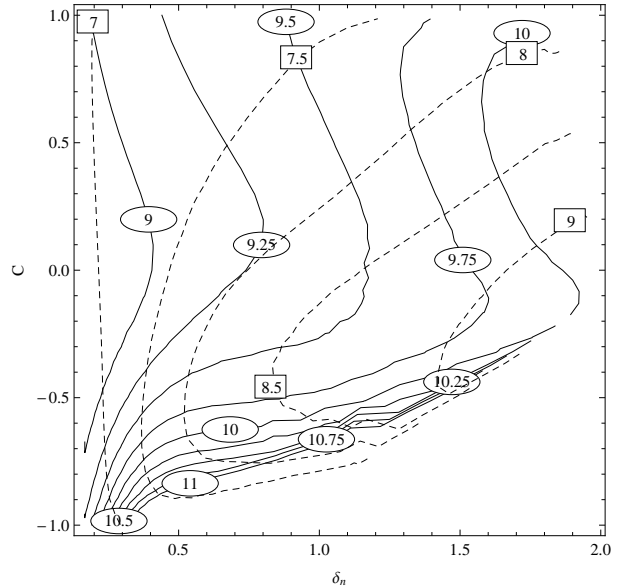


Figure 7. The isocontours of the numerical factor G in Eq. (35) for $\sigma_b = 1$ (dashed lines and labels in squares) and $\sigma_b \rightarrow \infty$ (solid lines and labels in ovals) shown in the (δ_n, C) -plane.

negative (i.e. $n_{\text{cr}} = 0$ wherever the model defined by Eq. (16) returns a negative value). The model has four free parameters:

- (i) the relative level of magnetic field fluctuations $\delta_b = \sigma_b/B_0$,
- (ii) the relative level of cosmic-ray number density fluctuations $\delta_n = \sigma_n/n_0$,
- (iii) the cross-correlation coefficient between magnetic field and cosmic rays C , and
- (iv) the dominant energy wave number of the turbulent magnetic field k_0 .

We do not vary the spectral index of magnetic field and cosmic rays as these parameters are of secondary importance in this context.

The value of k_0 controls the correlation lengths of magnetic field (Eq. (32)), cosmic rays and synchrotron emissivity, and hence the number of the correlation cells of synchrotron intensity fluctuations in the telescope beam N , which in turn affects the magnitude of synchrotron intensity fluctuation as $\delta_I \propto N^{-1/2}$. Since N can vary widely between different lines of sight in the Milky Way and between galaxies with different inclination angles, we present our results in terms of $N^{1/2}\delta_I$ for both the observations and the model.

6.2 A relation between the correlation lengths of the synchrotron emissivity and magnetic field

In the case of an infinitely narrow beam, the number of synchrotron correlation cells traversed by the emission is just the ratio $N = L/(2l_\varepsilon)$, where L is the path length through the synchrotron source and l_ε is the correlation length of the fluctuations in the synchrotron emissivity. For a finite beam width W , this is the number of correlation cells within the beam cylinder, $N \simeq (3/16)LW^2/l_\varepsilon^3$, assuming a circular beam and spherical correlation cells. Unlike the correlation lengths of physical parameters such as the magnetic field, velocity or density fluctuations, the correlation length of the intensity (or emissivity) variations cannot be deduced independently (e.g., from the nature of the turbulence driving), but has to be calculated from the statistical parameters of the physical variables or from ob-

servations. Here, we shall derive an expression for l_ε in terms of l_b , which will allow us also to estimate N .

To illustrate the difficulties arising, consider the autocorrelation function of b_\perp^2 as an example. If $V(x)$ is a stationary Gaussian random function, with vanishing mean value and the autocorrelation function $K_v(r) = \overline{V(x)V(x+r)}$, the autocorrelation function of $V^2(x)$ is given by $K_{v^2}(x) = 2[K_v(r)]^2$ (see e.g. §13 in Sveshnikov 1966). Assuming that each Cartesian vector component b_i of the random magnetic field \mathbf{b} is a Gaussian random variable, with the autocorrelation function K_{b_i} , we have $K_{b_i^2} = 2K_{b_i}^2$. Assuming statistical isotropy of \mathbf{b} , $K_{b_x}(r) = K_{b_y}(r)$, and neglecting any cross-correlations between b_x and b_y , we obtain the autocorrelation function of b_\perp^2 :

$$K_{b_\perp^2}(r) = 4K_{b_i}^2(r).$$

The relation between the correlation scales of b_i and b_\perp^2 , denoted l_{b_i} and $l_{b_\perp^2}$, respectively, depends on the form of the autocorrelation function of magnetic field: for $K_{b_i} = \frac{1}{3}\sigma_b^2 \exp(-r/l_b)$, we have $l_{b_\perp^2} = l_{b_i}/2$. However, for $K_{b_i} = \frac{1}{3}\sigma_b^2 \exp(-\pi r^2/l_b^2)$ we have $l_{b_\perp^2} = l_{b_i}/\sqrt{2}$. There is no universal relation between the correlation scales of even these simply connected variables. Such a relation should be established in each specific case from the statistical properties of each physical component of the system.

Since the power spectrum is a Fourier transform of the correlation function, these arguments also apply to the power spectra of b_i and ε .

We calculate the correlation length l_ε of the synchrotron emissivity $\varepsilon \propto n_{\text{cr}} B_\perp^2$ in the synthetic radio maps from its autocorrelation function $K_\varepsilon(r)$, for various values of the cross-correlation coefficients C , B_0 and n_0 :

$$l_\varepsilon = \sigma_\varepsilon^{-2} \left(\int_0^L K_\varepsilon(r) dr - \langle \varepsilon \rangle^2 \right), \quad (34)$$

where L is the path length and σ_ε is the standard deviation of the synchrotron emissivity (assuming $L \gg l_\varepsilon$ to minimize the impact of statistical fluctuations).

The resulting dependence of l_ε on the correlation length of the magnetic field l_b , obtained in Eq. (32) for the spectrum given by Eq. (30), can be approximated as

$$l_\varepsilon/L \approx G^{-1} (4l_b/L)^{0.65}, \quad (35)$$

where the numerical factor G depends on the model parameters and the cross-correlation coefficient C . The contours of G in the (δ_n, C) -plane are shown in Fig. 7; $G = 9$ – 10 are representative values for $\delta_b > 2$ – 3 , independent of the exact choice for δ_n provided $\delta_n \lesssim 1$. The resulting values of $N = L/(2l_\varepsilon)$ are used below to compare the synchrotron intensity fluctuations obtained from observations in Section 3 with the model of Section 5.

6.3 Correlation between cosmic rays and magnetic fields

The relative intensity of synchrotron intensity fluctuations is sensitive to the number N of correlation cells of synchrotron emissivity within the beam (or along the line of sight in case of a pencil beam). When comparing the theoretical model with observations, we adopt $L = 1$ kpc for the pathlength in the Milky Way, $l_{b_i} = 50$ pc for the correlation length of magnetic field, $\delta_b = 3$ (the asymptotic limit $\delta_b \gg 1$ is quite accurate in this case), and explore the range $-1 \leq C \leq 1$ for the cross-correlation coefficient between cosmic-ray and magnetic fluctuations. For $l_b/L = 0.05$ and $G \approx 9$ (see

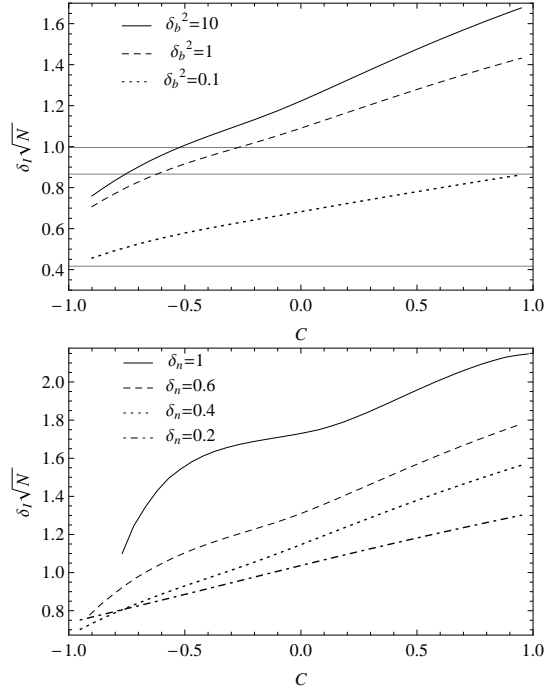


Figure 8. Relative fluctuations of the synchrotron intensity in synthetic radio maps of Section 6.1 versus the cross-correlation coefficient between B^2 and n_{cr} for various choices of the model parameters. Top panel: a selection of δ_b values for fixed $\delta_n = 0.5$ (solid: $\delta_b^2 = 10$; dashed: 1; dotted: 0.1). Grey horizontal lines correspond to uniformly distributed cosmic rays, $\delta_n = 0$, for the same values of δ_b (with δ_I decreasing with δ_b). Lower panel: various values of δ_n for $\delta_b^2 = 10$ ($\delta_n = 1$, solid; 0.6, dashed; 0.4, dotted; 0.2, dash-dotted).

Fig. 7), we have $l_\varepsilon \approx 40$ pc and $N = L/(2l_\varepsilon) \simeq 10$; we also discuss the effect of larger values of N .

Figure 8 shows the dependence of $\delta_I \sqrt{N}$ on the cross-correlation coefficient C for various values of the parameters δ_b and δ_n . The calculations are based on 100 realizations of \mathbf{B} , so the statistical errors of the mean values shown are negligible.

As can be seen from the upper panel of Fig. 8, the relative magnitude of synchrotron intensity fluctuations, $\delta_I \sqrt{N} > 0.7$, obtained for $\delta_b \geq 1$ and $\delta_n = 0.5$, is stronger than what is observed in the Milky Way, $\delta_I \sqrt{N} = 0.3$ – 0.6 assuming $N = 10$. If $N = 20$, the conservative observational estimate $\delta_I = 0.1$ – 0.2 translates into $\delta_I \sqrt{N} = 0.4$ – 0.9 , implying $C \lesssim -0.6$ for the highest $\delta_I \sqrt{N}$. Thus, $\delta_n < 0.5$ seems to be justified, unless N is significantly larger than 10 or, otherwise, $\delta_b < 1$ (which is highly implausible). Since the estimate $\delta_I = 0.1$ – 0.2 has been obtained for high Galactic latitudes, the path length is unlikely to be much longer than 1 kpc, and the correlation length of the synchrotron intensity fluctuations can hardly be much shorter than about 50 pc. Thus, excluding the case of simultaneously large L and small l_ε , we conclude that the distribution of cosmic ray electrons is unlikely to have any significant variations at scales of order 50–100 pc.

The lower panel in Fig. 8, where a range of values of δ_n are used with $\delta_b^2 = 10$, suggests that any positive correlation between cosmic rays and magnetic fields is only compatible with the observational estimate $\delta_I \sqrt{N} = 0.3$ – 0.6 (for $N = 10$) if $\delta_n < 0.2$. In fact, an upper limit $\delta_I \sqrt{N} = 0.9$ (for $N = 20$) might be achieved for $n_{\text{cr}} = \text{const}$. The values of $\delta_I \sqrt{N}$ in this case are shown with grey horizontal lines in the upper panel: for example, $\delta_I \sqrt{N} = 1$ is compatible with $\delta_b^2 = 10$. However, the lower values

of synchrotron intensity fluctuations in the Milky Way in the range $\delta_I \sqrt{N} = 0.3-0.9$ for $N = 10-20$ can be compatible with the presence of fluctuations in cosmic ray density mildly anticorrelated with those in magnetic field. It is difficult to be precise here, but $\delta_n < 0.2$ and $C < -0.5$ seems to be an acceptable combination of parameters.

7 PROPAGATION OF COSMIC RAYS AND EQUIPARTITION WITH MAGNETIC FIELDS

To illustrate the relation between cosmic rays and magnetic fields, consider a simple model of cosmic ray propagation near a magnetic flux tube. The number density of cosmic rays n_{cr} (or their energy density ϵ_{cr}) is assumed to obey the diffusion equation with the source Q and diffusivity D terms depending on the magnetic field (Parker 1969; Kuznetsov & Ptuskin 1983; Schlickeiser & Lerche 1985). Consider the steady state of a one-dimensional system with $Q = \text{const}$. The magnetic field is assumed to have a statistically uniform fluctuating component, $\overline{b^2} = \sigma_b^2 = \text{const}$, whereas the mean field is confined to a Gaussian slab of half-thickness L symmetric with respect to $x = 0$: $B_y = B_0 \exp[-x^2/(2d^2)]$, $B_x = B_z = 0$. The cosmic ray diffusivity is assumed to depend on the relative strength of magnetic fluctuations, $D = D_0 \sigma_b^2 / B_y^2$. The resulting steady-state diffusion equation

$$\frac{d}{dx} D \frac{d}{dx} n_{\text{cr}} + Q = 0,$$

can easily be solved with the boundary conditions

$$\frac{dn_{\text{cr}}}{dx}(0) = 0, \quad n_{\text{cr}}|_{|x| \rightarrow \infty} = 0,$$

to yield

$$n_{\text{cr}} = \frac{QB_0^2 d^2}{2D_0 \sigma_b^2} e^{-x^2/d^2}. \quad (36)$$

The total number (and energy) of cosmic rays remains finite despite the uniform distribution of their sources, $Q = \text{const}$, because $D \rightarrow \infty$ as $|x| \rightarrow \infty$ in this illustrative model.

This simple solution shows that, near a magnetic flux tube in a statistically homogeneous random magnetic field, cosmic rays concentrate where the total magnetic field is stronger because their diffusivity is smaller there. In this example, the spatial distributions of cosmic rays and magnetic field are tightly correlated.

Another type of argument relating cosmic ray energy density to parameters of the interstellar medium was suggested by Padoan & Scalo (2005). If both the magnetic flux and the cosmic ray flux are conserved, $BS = \text{const}$ and $n_{\text{cr}}US = \text{const}$ (where B is the magnetic field strength and S is the area within a fluid contour, and U is the cosmic ray streaming velocity), one obtains $n_{\text{cr}}U/B = \text{const}$, which yields $n_{\text{cr}} \propto n^{1/2}$, given that $U = V_A \propto Bn^{-1/2}$, with n the gas number density and V_A the Alfvén speed. Thus, the cosmic ray density is independent of the magnetic field strength, and scales with the thermal gas density. This result relies on the fact that the streaming velocity of the cosmic rays is proportional to the Alfvén speed. If, instead, $U = V$, with V the gas speed, we obtain $n_{\text{cr}} \propto B$ from these arguments. No clear scaling of the cosmic rays energy density ϵ_{cr} with the magnetic field was observed in the simulations of Snodin et al. (2006) who use the gas velocity for U . There is indication that the average propagation length of CREs depends on the degree of field ordering and hence varies between galaxies (Tabatabaei et al. 2013).

Assumption of a detailed, point-wise (local) equipartition between cosmic rays and magnetic fields is dubious also because these two quantities have vastly different diffusivities, and therefore cannot be similarly distributed in space. Magnetic filaments and sheets produced by the small-scale dynamo in the diffuse warm gas can have scales as small as a few parsecs (Shukurov 2007), and the strength of this turbulent magnetic field can be about $5 \mu\text{G}$. The large-scale magnetic field varies over scales of order 1 kpc, consistent with the turbulent diffusivity of $10^{26} \text{ cm}^2 \text{ s}^{-1}$ and time scale $5 \times 10^8 \text{ yr}$. The diffusive length scale of cosmic rays, based on the diffusivity of $D \simeq 10^{28} \text{ cm}^2 \text{ s}^{-1}$ and the confinement time in the disc, $\tau \simeq 10^7 \text{ yr}$, is about $(2D\tau)^{1/2} \simeq 1 \text{ kpc}$, similar to the length scale of the large-scale magnetic field. On these grounds, it is not impossible that the energy densities of cosmic rays and the *large-scale* magnetic field vary at similar scales, but this would be very implausible for the total magnetic field. Then equipartition arguments may be better applicable to observations of external galaxies, where the linear resolution is not better than a few hundred parsecs, than to the case of the Milky Way.

8 DISCUSSION

The general picture emerging from our results is that cosmic rays and magnetic fields are slightly anticorrelated at the relatively small, sub-kiloparsec scales explored here ($n_{\text{cr}} = \text{const}$ is also a viable possibility). Such an anticorrelation can result from statistical pressure equilibrium (i.e. a statistically constant total pressure) in the ISM, where cosmic rays and magnetic fields make similar contributions to the total pressure. An additional effect leading to an anticorrelation is the increase in the synchrotron losses of relativistic electrons in stronger magnetic field.

Strictly speaking, this conclusion applies to regions for which we have analysed the data: high Galactic latitudes in the Milky Way and the outer parts of M33. However, it is likely that this result reflects general features of cosmic ray propagation.

Local energy equipartition (or pressure equality) between cosmic rays and magnetic field would produce stronger fluctuations of synchrotron intensity than those observed. However, equipartition between cosmic rays and magnetic field cannot be excluded at larger scales of order 1 kpc and greater. Hoernes et al. (1998) indirectly make a similar conclusion concerning loss of equipartition at small scales from their analysis of the radio–far-infrared correlation in M31.

Since magnetic fields and cosmic rays have vastly different diffusivities, and therefore, must vary at very different scales, any strong correlation between them can hardly be expected at scales smaller than 1 kpc. Correlated (or rather anticorrelated) fluctuations can, however, arise from such secondary processes as the adjustment to pressure equilibrium, etc.

Our arguments and conclusions are based on observations and modelling of synchrotron emission, a tracer of the electron component of cosmic rays. Thus, our conclusions strictly apply only to the cosmic ray electrons. However, the only significant difference between the behaviour of electrons and protons in this context is that the former experience higher energy losses due to synchrotron emission and inverse Compton scattering off the relic microwave photons. The energy loss time scale $\simeq 4 \times 10^8 \text{ yr} (E/1 \text{ GeV})^{-1}$ in a magnetic field of $5 \mu\text{G}$ in strength, for particles emitting at wavelengths larger than 1 cm, is much longer than the confinement time 10^7 yr , so the energy losses are negligible unless the local magnetic field is unusually strong. Therefore, we extend our con-

clusions derived from analysis of synchrotron intensity fluctuations to cosmic rays as a whole. Moreover, energy losses can only make the distribution of the electrons more inhomogeneous than that of the protons, so that our conclusions are robust with respect to this caveat.

Our model, data and their analysis arguably match each other in the level of detail. We do not include any latitudinal variation of the path length L and the variation of the angular size of the turbulent cells, l_0/L with Galactic latitude in the Milky Way. Instead, we restrict our analysis to the range $|b| > 30^\circ$ within which both l_0/L and L vary by a factor of two. The important parameter, the square root of the number of turbulent cells along the path length, $N^{1/2} \simeq (L/2l_0)^{1/2}$ then varies by a factor of about 1.5. Since there are other parameters varying with galactic latitude (e.g., the magnitudes of the random and regular magnetic fields, cosmic-ray intensity, etc.), including the dependence of the path length and the correlation scale into the model would make it significantly more complicated, if possible at all. Therefore, we prefer, instead, to present our results in the form of plausible ranges that allow for the numerous effects that remain beyond the framework of the model.

To simplify analytical calculations, we have adopted $s = -1$ for the synchrotron spectrum, so that the synchrotron emissivity ε is proportional to $B_\perp^{1-s} = B_\perp^2$. We have verified that numerical results obtained with the more commonly used value $s = -0.7$, where $\varepsilon \propto B_\perp^{1.7}$, differ insignificantly from those with $s = -1$.

Our model includes magnetic field and cosmic ray distributions represented by a wide range of scales, with the magnetic energy spectrum given by Eq. (30). However, the spectral index of magnetic fluctuations only appears in the expressions for the r.m.s. magnetic field fluctuations, Eq. (31), and the magnetic correlation length, Eq. (32), through which it affects the number of correlation cells N . Otherwise, the standard deviation of the synchrotron intensity is not sensitive to the magnetic spectrum.

We have adopted $l_0 = 50\text{--}100$ pc for the correlation scale of the random magnetic field. Estimates of the turbulent scales in the magnetoionic medium of the Milky Way are numerous and divergent. Ruzmaikin & Sokoloff (1977) discuss in detail techniques for estimating turbulent scales from pulsar RM data and obtain $l_0 = 100\text{--}150$ pc without any restrictive assumptions regarding the correlation between the fluctuations in magnetic field and thermal electrons. Rand & Kulkarni (1989) estimate the size of a turbulent cells as $2l_0 = 55$ pc (using our notation) from the Faraday rotation measures of pulsars. In fact, their result refers to the size of the correlation cell of RM fluctuations and these authors do not discuss how it is related to the correlation scale of magnetic field; this relation depends on the degree of (anti) correlation between the fluctuation in magnetic field and thermal electron density (Beck et al. 2003). Ohno & Shibata (1993) estimate the scale of magnetic field fluctuations from the RM of close pairs of pulsars to obtain $2l_0 = 10\text{--}100$ pc. Their model includes fluctuations in thermal electron density but they are, presumably, considered to be uncorrelated with magnetic field fluctuations; this assumption can significantly affect the result. Haverkorn et al. (2008) obtain the integral (correlation) scale from RM and depolarization of extragalactic radio sources; their sample probes the inner Galaxy avoiding its central part. These authors obtain $l_0 = 1\text{--}5$ pc from the Faraday rotation measures and $l_0 = 3.5\text{--}8.7$ pc from depolarization. The authors attribute the difference from other estimates of the outer scale to a correspondingly smaller energy input scale of interstellar turbulence of a few parsecs. Perhaps more plausibly, the fluctuations in RM, depolarization or any other parameter

can have a hierarchy of characteristic scales due, say, to interstellar shocks, intermittent small-scale magnetic filaments, etc., and different methods can be sensitive to only some of them. Fletcher et al. (2011) deduce the correlation scale of RM fluctuations from high-resolution observations of M51 by comparing the scatter in the values of RM observed under various degrees of spatial smoothing and assuming that the standard deviation of RM scales as $l_0^{1/2}$ as predicted by theory (e.g., Sokoloff et al. 1998). The resulting scale of RM fluctuations is $l_{\text{RM}} = 50$ pc. Houde et al. (2013) analysed the dispersion of synchrotron polarisation angles in high-resolution observations of M51 to estimate $l_0 = 98 \pm 5$ pc and $l_0 = 54 \pm 3$ pc parallel and perpendicular to the local mean-field direction respectively.

We discuss the relation between the correlation lengths of synchrotron intensity and magnetic field in Section 6.2; this discussion and conclusions apply to other observables as well. It is important that there is no universal relation between the correlation lengths of, say, B_\perp^2 and B : to establish such a relation, one has to know the auto-correlation functions of B_\perp and B_\parallel . In addition, such observables as Faraday rotation measure, total or polarized radio intensity involve not only magnetic field but also number densities of thermal or relativistic electrons. The cross-correlation between these variables and magnetic field are also required to deduce the statistical properties of magnetic field. The comprehensive statistical analysis is recently suggested by Lazarian & Pogosyan (2012). However the theoretical predictions discussed there is hardly possible to compare with available observational data. Only the simplest statistical characteristics give robust results.

Our results can significantly change the interpretation of high-resolution radio observations of the Milky Way and spiral galaxies. Present interpretations, aimed at estimating the strength and geometry of interstellar magnetic fields, rely heavily on the assumption of local equipartition between cosmic rays and magnetic fields, at a scale corresponding to the resolution of the observations. This assumption is acceptable if the resolution is not finer than the diffusion length of the cosmic rays, about say, 1 kpc. However, this assumption is questionable when applied to observations at higher resolution. We suggest a different procedure to interpret such observations. The original total intensity radio maps should first be smoothed to the scale of the cosmic ray distribution, 1 kpc, where the equipartition assumption *may* apply, and the distribution of cosmic rays can be deduced from the smoothed data. (The smoothing length may depend on the local environment e.g. star formation rate, magnetic field etc. — this requires further investigation using suitable cosmic ray propagation models.) After that, this distribution of cosmic rays can be used to deduce the magnetic field distribution from the data at the original resolution. Since a larger part of the synchrotron intensity fluctuations observed will be attributed to magnetic fields, it is clear that this procedure will result in a more inhomogeneous magnetic field than that arising from the assumption of local equipartition so often used now.

ACKNOWLEDGMENTS

We thank an anonymous referee for a careful and insightful report on the submitted version of the paper, which resulted in many improvements. We are also grateful to Wolfgang Reich for helpful comments. Financial support from the Royal Society and Newcastle University is gratefully acknowledged. At various stages, this work was supported by the Leverhulme Trust under Research Grant RPG-097, the Royal Society, and by the National Science Founda-

tion under Grant NSF PHY05-51164. RS acknowledges support from the grant YD-520.2013.2 of the Council of the President of the Russian Federation. Numerical simulations were partially performed on the supercomputer "URAN" of Institute of Mathematics and Mechanics UrB RAS.

APPENDIX A: THE MEAN AND STANDARD DEVIATION OF THE SYNCHROTRON INTENSITY

Here we derive analytical expressions for magnitude of relative synchrotron intensity fluctuations $\delta_I = \sigma_I/I_0$, with σ_I the standard deviation of the synchrotron intensity I and I_0 , its mean value. Relations between the statistical characteristics of synchrotron intensity and synchrotron emissivity $\varepsilon = n_{cr}B_{\perp}^2$ are given by Eqs. (12) and (14). Here we calculate $\bar{\varepsilon}$ and $\sigma_{\varepsilon}^2 = \overline{\varepsilon^2} - \bar{\varepsilon}^2$ using the cosmic ray model, partially correlated with magnetic fields, introduced in Section 4.2. Here overbar denotes ensemble averaging. The calculations are quite straightforward although somewhat cumbersome.

We start with calculating $\bar{\varepsilon}$ using n_{cr} from Eq. (23):

$$\begin{aligned} \bar{\varepsilon} &= \overline{n_{cr}B_{\perp}^2} \\ &= n_0 \overline{B_{\perp}^2} + \frac{\sigma_n C}{\sigma_{B^2}} (\overline{B^2 B_{\perp}^2} - \overline{B^2} \overline{B_{\perp}^2}) \\ &\quad + \frac{\sigma_n \sqrt{1-C^2}}{\sigma_F} (\overline{F B_{\perp}^2} - \overline{F} \overline{B_{\perp}^2}). \end{aligned}$$

The last term vanishes since F and B_{\perp}^2 are uncorrelated by construction, and hence $\overline{F B_{\perp}^2} = \overline{F} \overline{B_{\perp}^2}$ and $\overline{F B_{\perp}^2} = \overline{F} \overline{B_{\perp}^2}$. For the same reason, all terms in ε^2 that contain F also vanish.

As each Cartesian vectorial component of the random magnetic field \mathbf{b} is assumed to be a Gaussian random variable with zero mean value, $\bar{b}_i = 0$, we have, for the higher statistical moments,

$$\overline{b_i^{2k}} = \frac{(2k)!}{2^k k!} \sigma_b^{2k}, \quad \overline{b_i^{2k+1}} = 0, \quad k = 1, 2, \dots, \quad (\text{A1})$$

where $i = x, y, z$. This allows us to calculate the higher-order moments that contribute to $\bar{\varepsilon}$ and $\overline{\varepsilon^2}$ as follows:

$$\begin{aligned} \overline{B_{\perp}^4} &= B_{0\perp}^4 + \frac{8}{3} B_{0\perp}^2 \sigma_b^2 + \frac{8}{9} \sigma_b^4, \\ \overline{B^4} &= B_{0\perp}^4 + \frac{10}{3} B_{0\perp}^2 \sigma_b^2 + \frac{5}{3} \sigma_b^4 \\ &\quad + 2B_{0\perp}^2 B_{0\parallel}^2 + \frac{10}{3} B_{0\parallel}^2 \sigma_b^2 + B_{0\parallel}^4 \\ \overline{B^2 B_{\perp}^4} &= B_{0\perp}^4 B_{0\parallel}^2 + \frac{8}{3} B_{0\perp}^2 \sigma_b^2 B_z^2 + \frac{8}{9} \sigma_b^4 B_{0\parallel}^2 \\ &\quad + B_{0\perp}^6 + \frac{19}{3} B_{0\perp}^4 \sigma_b^2 + \frac{80}{9} B_{0\perp}^2 \sigma_b^4 + \frac{56}{27} \sigma_b^6, \\ \overline{B^4 B_{\perp}^4} &= 2B_{0\perp}^6 B_{0\parallel}^2 + 14B_{0\perp}^4 \sigma_b^2 B_{0\parallel}^2 + B_{0\perp}^4 B_{0\parallel}^4 \\ &\quad + \frac{64}{3} B_{0\perp}^2 \sigma_b^4 B_{0\parallel}^2 + \frac{8}{3} B_{0\perp}^2 \sigma_b^2 B_{0\parallel}^4 \\ &\quad + \frac{16}{3} \sigma_b^6 B_{0\parallel}^2 + \frac{8}{9} \sigma_b^4 B_{0\parallel}^4 + B_{0\perp}^8 + \frac{34}{3} B_{0\perp}^6 \sigma_b^2 \\ &\quad + \frac{109}{3} B_{0\perp}^4 \sigma_b^4 + \frac{104}{3} B_{0\perp}^2 \sigma_b^6 + \frac{56}{9} \sigma_b^8. \end{aligned}$$

The algebra involved in deriving these relations is rather daunting; we used symbolic algebra software to derive these relations.

We finally have from Eqs. (12), (14) and (23):

$$I_0 = \frac{n_0 N l_{\varepsilon}}{9} [4C \sigma_{B^2}^{-1} \delta_n \sigma_b^4 + 6\sigma_b^2 + 3(4C \sigma_{B^2}^{-1} \delta_n \sigma_b^2 + 3) B_{0\perp}^2], \quad (\text{A2})$$

and

$$\begin{aligned} \sigma_I^2 &= \frac{n_0^2 N l_{\varepsilon}^2}{81} \left\{ 224C^2 \sigma_{B^2}^{-2} \delta_n^2 \sigma_b^8 - 81\delta_n^2 (C^2 - 1) B_{0\perp}^4 + 2\sigma_b^4 \right. \\ &\quad + 18\sigma_b^4 [51C^2 \sigma_{B^2}^{-2} \delta_n^2 B_{0\perp}^4 + 36C \sigma_{B^2}^{-1} \delta_n B_{0\perp}^2 - 4\delta_n^2 (C^2 - 1)] \\ &\quad + 12C^2 B_{0\parallel}^2 \frac{\sigma_b^2}{\sigma_{B^2}^2} \delta_n^2 (9B_{0\perp}^4 + 24\sigma_b^2 B_{0\perp}^2 + 8\sigma_b^4) \\ &\quad + 108B_{0\perp}^2 \sigma_b^2 [(C \sigma_{B^2}^{-1} \delta_n B_{0\perp}^2 + 1)^2 - 2\delta_n^2 (C^2 - 1)] \\ &\quad \left. + 144C \sigma_{B^2}^{-1} \delta_n (9C \sigma_{B^2}^{-1} \delta_n B_{0\perp}^2 + 1) \sigma_b^6 \right\}, \quad (\text{A3}) \end{aligned}$$

where

$$\sigma_{B^2}^2 = \overline{B^4} - \overline{B^2}^2 = B_0^4 + \frac{10}{3} B_0^2 \sigma_b^2 + 3\sigma_b^4. \quad (\text{A4})$$

REFERENCES

- Abdo A. A. et al., 2010, *A&A*, 512, A7
 Arbutina B., Urošević D., Andjelić M. M., Pavlović M. Z., Vukotić B., 2012, *ApJ*, 746, 79
 Arshakian T. G., Stepanov R., Beck R., Krause M., Sokoloff D., 2011, *Astron. Nachr.* 332, 524
 Banday A. J., Giller M., Wolfendale A. W., 1991a, in *The 22nd International Cosmic Ray Conference*, Vol. 2, p. 736
 Banday A. J., Wolfendale A. W., Giler M., Szabelska B., Szabelski J., 1991b, *ApJ*, 375, 432
 Beck R., 2007, *A&A*, 470, 539
 Beck R., Brandenburg A., Moss D., Shukurov A., Sokoloff D., 1996, *ARAA*, 34, 155
 Beck R., Fletcher A., Shukurov A., Snodin A., Sokoloff D. D., Ehle M., Moss D., Shoutenkov V., 2005, *A&A*, 444, 739
 Beck R., Krause M., 2005, *Astron. Nachr.*, 326, 414
 Beck R., Shukurov A., Sokoloff D., Wielebinski R., 2003, *A&A*, 411, 99
 Berezhinskii V. S., Bulanov S. V., Dogel V. A., Ginzburg V. L., Ptuskin V. S., 1990, *Astrophysics of Cosmic Rays*. North-Holland, Amsterdam
 Beuermann K., Kanbach G., Berkhuijsen E. M., 1985, *A&A*, 153, 17
 Bridle A. H., 1967, *MNRAS*, 136, 219
 Burbidge G. R., 1956a, *ApJ*, 124, 416
 Burbidge G. R., 1956b, *ApJ*, 123, 178
 Burn B. J., 1966, *MNRAS*, 133, 67
 Carilli C. L., Taylor G. B., 2002, *ARAA*, 40, 319
 Casse F., Lemoine M., Pelletier G., 2002, *Phys. Rev. D*, 65, 023002
 Chi X., Wolfendale A. W., 1993, *Nat*, 362, 610
 Christenson M., Hindmarsh M., Brandenburg A., 2001, *Phys. Rev. E*, 64, 056405
 Chyży K. T., 2008, *A&A*, 482, 755
 Dagkesamanskii R. D., Shutenkov V. R., 1987, *Sov. Astron. Lett.*, 13, 73
 Fletcher A., Beck R., Shukurov A., Berkhuijsen E. M., Horellou C., 2011, *MNRAS*, 412, 2396
 Galtier S., Nazarenko S. V., Newell A. C., Pouquet A., 2000, *J. Plasma Phys.*, 63, 447
 Gent F. A., Shukurov A., Sarson G. R., Fletcher A., Mantere M. J., 2013, *MNRAS*, 430, L40
 Getmantsev G. G., 1959, *Sov. Astron.*, 3, 415
 Giacalone J., Jokipii J. R., 1999, *ApJ*, 520, 204
 Goldreich P., Sridhar S., 1995, *ApJ*, 438, 763

- Haslam C. G. T., Salter C. J., Stoffel H., Wilson W. E., 1982, *A&AS*, 47, 1
- Haverkorn M., Brown J. C., Gaensler B. M., McClure-Griffiths N. M., 2008, *ApJ*, 680, 362
- Hoernes P., Berkhuijsen E. M., Xu C., 1998, *A&A*, 334, 57
- Houde M., Fletcher A., Beck R., Hildebrand R. H., Vaillancourt J. E., Stil J. M., 2013, *ApJ*, 766, 49
- Kuznetsov V. D., Ptuskin V. S., 1983, *Ap&SS*, 94, 5
- La Porta L., Burigana C., Reich W., Reich P., 2008, *A&A*, 479, 641
- Laing R. A., 1980, *MNRAS*, 193, 439
- Lawson K. D., Mayer C. J., Osborne J. L., Parkinson M. L., 1987, *MNRAS*, 225, 307
- Lazarian A., Pogosyan D., 2012, *ApJ*, 747, 5
- Lithwick Y., Goldreich P., Sridhar S., 2007, *ApJ*, 655, 269
- Longair M. S., 1994, *High energy astrophysics. Vol.2: Stars, the galaxy and the interstellar medium.* Cambridge: Cambridge University Press, 2nd ed.
- Malik N. A., Vassilicos J. C., 1999, *Phys. Fluids*, 11, 1572
- Mao S. A. et al., 2012, *ApJ*, 759, 25
- Mills B. Y., Slee O. B., 1957, *Austr. J. Phys.*, 10, 162
- Monin A., Yaglom A., 1975, *Statistical Fluid Mechanics: Mechanics of Turbulence*, vol. 2. MIT Press, Cambridge, Mass
- Moss D., Stepanov R., Arshakian T. G., Beck R., Krause M., Sokoloff D., 2012, *A&A*, 537, A68
- Ohno H., Shibata S., 1993, *MNRAS*, 262, 953
- Oppermann N., Junklewitz H., Robbers G., Enßlin T. A., 2011, *A&A*, 530, A89
- Orienti M., Dallacasa D., 2008, *A&A*, 487, 885
- Padoan P., Scalo J., 2005, *ApJ*, 624, L97
- Parker E. N., 1966, *ApJ*, 145, 811
- Parker E. N., 1969, *Space Sci. Rev.*, 9, 651
- Parker E. N., 1979, *Cosmical magnetic fields: Their origin and their activity.* Oxford, Clarendon Press,
- Pohl M., 1993, *A&A*, 279, L17
- Rand R. J., Kulkarni S. R., 1989, *ApJ*, 343, 760
- Readhead A. C. S., 1994, *ApJ*, 426, 51
- Roger R. S., Costain C. H., Landecker T. L., Swerdlyk C. M., 1999, *A&AS*, 137, 7
- Rogstad D. H., Wright M. C. H., Lockhart I. A., 1976, *ApJ*, 204, 703
- Ruzmaikin A. A., Shukurov A. M., Sokoloff D. D., 1988, *Magnetic Fields of Galaxies.* Kluwer, Dordrecht
- Ruzmaikin A. A., Sokoloff D. D., 1977, *Ap&SS*, 52, 365
- Scheuer P. A. G., Williams P. J. S., 1968, *ARAA*, 6, 321
- Schlickeiser R., Lerche I., 1985, *A&A*, 151, 151
- Scott M. A., Readhead A. C. S., 1977, *MNRAS*, 180, 539
- Shukurov A., 2007, in *Mathematical Aspects of Natural Dynamios*, Dormy E., Soward A. M., eds., London, Chapman and Hall/CRC, pp. 313–359
- Slish V. I., 1963, *Nat*, 199, 682
- Snodin A. P., Brandenburg A., Mee A. J., Shukurov A., 2006, *MNRAS*, 373, 643
- Sokoloff D. D., Bykov A. A., Shukurov A., Berkhuijsen E. M., Beck R., Poezd A. D., 1998, *MNRAS*, 299, 189
- Stepanov R., Arshakian T. G., Beck R., Frick P., Krause M., 2008, *A&A*, 480, 45
- Stepanov R., Fletcher A., Shukurov A., Beck R., La Porta L., Tabatabaei F. S., 2009, in *IAU Symposium*, Vol. 259, pp. 93–94
- Stil J. M., Krause M., Beck R., Taylor A. R., 2009, *ApJ*, 693, 1392
- Sveshnikov A. A., 1966, *Applied Methods of the Theory of Random Functions.* Elsevier, Amsterdam
- Tabatabaei F. S., Beck R., Krügel E., Krause M., Berkhuijsen E. M., Gordon K. D., Menten K. M., 2007b, *A&A*, 475, 133
- Tabatabaei F. S., Berkhuijsen E. M., Frick P., Beck R., Schinnerer E., 2013, accepted in *A&A*, arXiv:1307.6253
- Tabatabaei F. S., Krause M., Beck R., 2007a, *A&A*, 472, 785
- Tabatabaei F. S., Krause M., Fletcher A., Beck R., 2008, *A&A*, 490, 1005
- Volegova A. A., Stepanov R. A., 2010, *JETP Lett.*, 90, 637
- Wilkin S. L., Barenghi C. F., Shukurov A., 2007, *Phys. Rev. Lett.*, 99, 134501
- Williams P. J. S., 1963, *Nat*, 200, 56